

Electronic Thesis and Dissertation Repository

12-3-2019 10:00 AM

Junctophilin-2 Protects Cardiomyocytes against Palmitate-induced Injury

Xiaoyun Ji
The University of Western Ontario

Supervisor
Peng, Tianqing
The University of Western Ontario Co-Supervisor
Jones, Douglas
The University of Western Ontario

Graduate Program in Pathology
A thesis submitted in partial fulfillment of the requirements for the degree in Master of Science
© Xiaoyun Ji 2019

Follow this and additional works at: <https://ir.lib.uwo.ca/etd>



Part of the [Cardiovascular Diseases Commons](#)

Recommended Citation

Ji, Xiaoyun, "Junctophilin-2 Protects Cardiomyocytes against Palmitate-induced Injury" (2019). *Electronic Thesis and Dissertation Repository*. 6743.
<https://ir.lib.uwo.ca/etd/6743>

This Dissertation/Thesis is brought to you for free and open access by Scholarship@Western. It has been accepted for inclusion in Electronic Thesis and Dissertation Repository by an authorized administrator of Scholarship@Western. For more information, please contact wlsadmin@uwo.ca.

Abstract

Cardiac lipotoxicity may induce cardiomyocyte apoptosis, eventually leading to myocardial dysfunction and heart failure. This study investigated whether and how junctophilin-2 (JPH2) plays a role in palmitate-induced apoptosis in cardiomyocytes. Here, we found palmitate incubation reduced JPH2 protein levels, increased cytosolic Ca^{2+} and induced apoptosis in cardiomyocytes. JPH2 over-expression prevented the increased cytosolic Ca^{2+} and apoptosis in palmitate-stimulated cardiomyocytes. JPH2 over-expression also attenuated palmitate-induced CCAAT-enhancer-binding protein homologous protein (CHOP) expression and CHOP deletion alleviated palmitate-induced apoptosis. Furthermore, blocking Ca^{2+} release from ryanodine receptor-2 (RyR2) prevented palmitate-stimulated CHOP induction and apoptosis. Additionally, JPH2 silencing elevated cytosolic Ca^{2+} , induced CHOP expression and apoptosis in cardiomyocytes; these effects of JPH2 silencing were inhibited by blocking Ca^{2+} release from RyR2. In summary, we demonstrate that JPH2 attenuates palmitate-induced apoptosis by reducing Ca^{2+} release from RyR2 and preventing CHOP expression in cardiomyocytes. Thus, targeting JPH2 may represent a new therapeutic strategy to treat cardiac lipotoxicity.

Keywords: Cardiomyocyte; Junctophilin-2; Palmitate; Apoptosis; Ca^{2+} ; CHOP; Ryanodine receptor-2; Cardiac lipotoxicity.

Summary for Lay Audience

The heart has both the greatest caloric needs and the most robust consumption of fatty acids of the human organs. Under certain abnormal or disease conditions, heart muscle cells get more fatty acids than they need and thus, the heart accumulates lipids. Excess lipids can directly damage heart muscle cell structures, resulting in the heart not working properly, a condition described as "cardiac lipotoxicity". Two human metabolic disorders are caused by excess lipid accumulation in heart muscle cells: obesity-related heart muscle disease in association with sudden heart death, and diabetic heart disease. The outcomes of cardiac lipotoxicity include severe heart impairment leading to death or needing replacement of the heart. Since type-2 diabetes and obesity are very common, cardiac lipotoxicity represents a major public health concern. However, effective treatments are limited for patients, which represents a major gap in patient care. Thus, further researches are urgently needed to better understand this disease, identify new targets for treatment and develop effective treatment modalities.

The objective of this study was to understand how a protein called "junctophilin-2" is involved in cardiac lipotoxicity. Since the levels of this junctophilin-2 protein are reduced in heart muscle cells during lipotoxicity, we examined whether addition of junctophilin-2 reduces heart muscle cell death caused by palmitate, a toxic lipid that has been widely applied in the study of cardiac lipotoxicity. It is well known that junctophilin-2 is important in maintaining a structure within cells which delivers ions (e.g. calcium) signals to force-generating fibers in heart muscle cells, leading to contraction. We examined how junctophilin-2 normalizes calcium signals and inhibits the occurrence of a condition called "endoplasmic reticulum stress", which causes heart muscle cell death under over-supply of palmitate. Thus, this study will identify new targets for treatment.

Acknowledgments

First and foremost, I would like to express my deepest gratitude to my supervisor, Dr. Tianqing Peng, for providing me the opportunity to pursue my master's degree at Western University. I have been extremely lucky to have a supervisor who cared so much about my work. Thank you for all your important advices to apply not only within the lab but also in life. This thesis could not have been completed without your significant patience and continued guidance.

I would like to extend my sincere gratitude to my co-supervisor, Dr. Douglas Jones, who facilitated my research and helped me all the way. Your valuable suggestions, constructive criticism and precious encouragement inspired me to get through tough times during my project.

Besides my mentors, I would like to acknowledge my advisory committee members, Dr. Chandan Chakraborty and Dr. Peter Basile Stathopoulos. I always felt like you were truly interested in and cared about my work and that you also wanted me to succeed. This meant a lot, and I greatly appreciate it. I would also like to thank members of the examination committee, Dr. Zia Khan, Dr. Zhu-xu Zhang and Dr. Patrick Lajoie, for their insight, constructive suggestions and recommendations.

My colleagues helped tremendously throughout my thesis. Particularly, I would like to acknowledge Dr. Dong Zheng whose expertise and support helped me in learning experiment techniques. Dr. Ting Cao gave me endless support and warm encouragement. Dr. Rui Ni, Rebecca Dang, Nima Nalin and Liwen Liang also offered me a lot of help. Special thanks are extended to Dr. Peter Basile Stathopoulos and Matthew Joseph Novello for their immeasurable help in the calcium experiment.

Last but not the least, I would like to acknowledge the Department of Pathology and Laboratory Medicine. Tracy and Susan, I deeply appreciate your extensive work to make the examination

happen. I am indebted to you for all your patient help. Dr. Zia Khan and Dr. Chandan Chakraborty, participating in your journal club courses not only expanded my horizon but also enlightened my thesis.

Dedication

I dedicate this to my father Wensheng Ji, my mother Yongmei Liu and my brother Yuan Ji.

Table of Contents

Abstract.....	ii
Summary for Lay Audience.....	iii
Acknowledgments.....	iv
Dedication.....	vi
List of Tables	xi
List of Figures.....	xii
Chapter 1.....	1
1 Introduction.....	1
1.1 Cardiac lipotoxicity.....	1
1.2 Junctophilin-2	3
1.2.1 JPH2 in T-tubule maturation.....	5
1.2.2 JPH2 in the postnatal development of junctional membrane complexes (JMCs)	6
1.2.3 JPH2-mediated regulation of RyR2.....	6
1.2.4 Regulation of JPH2 in cardiomyocytes.....	7
1.2.5 JPH2 encodes transcription regulator under stress	9
1.3 Endoplasmic reticulum stress	10
1.3.1 Unfolded protein response (UPR).....	11
1.3.2 Calcium homeostasis and ER stress.....	12
1.3.3 ER stress and apoptosis.....	13
1.3.4 ER stress in cardiovascular diseases	14
1.4 Apoptosis in cardiomyocytes.....	15
1.4.1 Apoptosis: programmed cell death	15
1.4.2 Apoptosis in cardiac lipotoxicity	18

1.5 Rationale	21
1.6 Hypothesis.....	22
1.7 Specific aims.....	22
1.7.1 To confirm that palmitate induces cell injury in cardiomyocytes.....	22
1.7.2 To determine if JPH2 knockdown enhances whereas JPH2 over-expression attenuates palmitate-induced cell injury in cardiomyocytes...	22
1.7.3 To determine the mechanism by which JPH2 protects cardiomyocytes against palmitate-induced injury by modulating calcium release from RyR2 and inhibiting ER stress.....	22
Chapter 2.....	23
2 Materials and Methods.....	23
2.1 Animals.....	23
2.2 Isolation and culture of neonatal mouse cardiomyocytes.....	24
2.3 Adenoviral infection.....	26
2.4 Sodium dodecyl sulphate-polyacrylamide gel electrophoresis (SDS-PAGE) and western blot analysis.....	27
2.5 Caspase-3 activity measurement.....	30
2.6 Cellular DNA fragmentation measurement.....	31
2.7 Oleate/Palmitate (OA/PA) solution preparation.....	33
2.8 Cytoplasmic free Ca ²⁺ detection.....	33
2.9 Statistical analysis.....	34
Chapter 3.....	37
3 Results.....	37
3.1 Palmitate incubation increases caspase-3 activity in cultured neonatal mouse cardiomyocytes.....	37
3.2 Palmitate incubation increases DNA fragmentation in cultured neonatal mouse cardiomyocytes.....	39
3.3 Palmitate incubation reduces JPH2 expression in cultured neonatal mouse cardiomyocytes.....	41

3.4 Knockdown of JPH2 in cultured neonatal mouse cardiomyocytes	43
3.5 JPH2 knockdown enhances palmitate-induced caspase-3 activity in cultured neonatal mouse cardiomyocytes	45
3.6 JPH2 knockdown enhances palmitate-induced DNA fragmentation in cultured neonatal mouse cardiomyocytes	47
3.7 Over-expression of JPH2 in cultured neonatal mouse cardiomyocytes.....	49
3.8 JPH2 over-expression attenuates palmitate-induced caspase-3 activity in cultured neonatal mouse cardiomyocytes	51
3.9 JPH2 over-expression attenuates palmitate-induced DNA fragmentation in cultured neonatal mouse cardiomyocytes	53
3.10 Knockdown of JPH2 induces caspase-3 activity in cultured neonatal mouse cardiomyocytes	55
3.11 Knockdown of JPH2 increases DNA fragmentation in cultured neonatal mouse cardiomyocytes	57
3.12 Palmitate incubation increases CHOP expression in cultured neonatal mouse cardiomyocytes	59
3.13 JPH2 knockdown increases CHOP expression in cultured neonatal mouse cardiomyocytes	61
3.14 Over-expression of JPH2 attenuates palmitate-induced CHOP expression in cultured neonatal mouse cardiomyocytes	63
3.15 CHOP knockout reduces JPH2 knockdown-induced caspase-3 activity in cultured neonatal mouse cardiomyocytes	65
3.16 CHOP knockout reduces palmitate-induced caspase-3 activity in cultured neonatal mouse cardiomyocytes.....	67
3.17 Inhibition of Ca ²⁺ release from RyR2 reduces palmitate-induced CHOP expression in cultured neonatal mouse cardiomyocytes.....	69
3.18 Inhibition of Ca ²⁺ release from RyR2 reduces JPH2 knockdown-induced CHOP expression in cultured neonatal mouse cardiomyocytes.....	71
3.19 Inhibition of Ca ²⁺ release from RyR2 reduces palmitate-induced apoptosis in cultured neonatal mouse cardiomyocytes	73
3.20 Ryanodine reduces palmitate-induced Ca ²⁺ release in cultured neonatal mouse cardiomyocytes	75

3.21 JPH2 over-expression attenuates palmitate-induced Ca ²⁺ release in cultured neonatal mouse cardiomyocytes	77
Chapter 4	79
4 Discussion, Limitations and Future Directions	79
4.1 Discussion	79
4.1.1 Palmitate-mediated down-regulation of JPH2 in cardiomyocytes.....	79
4.1.2 Novel cardiac protection of JPH2 against palmitate-induced apoptosis...	81
4.1.3 JPH2 prevention of ER stress in cardiomyocytes during lipotoxicity	82
4.1.4 Concluding remarks	84
4.2 Limitations and future directions	85
References	86
Curriculum Vitae	97

List of Tables

Table 1: Components of Solution A (100mL)	23
Table 2: Components of Solution B (100mL)	24
Table 3: Components of PCR System (25 μ L)	24
Table 4: Protocol of PCR for CHOP ^{-/-} Mouse	24
Table 5: Components of D-Hanks (1L)	26
Table 6: Components of Lysis Buffer (100 mL)	27
Table 7: Components of 6X Loading Buffer (100 mL)	27
Table 8: Components of Resolving Gel (10mL).....	28
Table 9: Components of Stacking Gel (3mL).....	28
Table 10: Components of Running Buffer (1L)	29
Table 11: Components of Transfer Buffer (1L).....	29
Table 12: Components of TBST (1L).....	30
Table 13: Components of Enhanced Chemiluminescence (ECL) Reagent (100mL).....	30
Table 14: Antibody Information for Western Blot	30
Table 15: Components of Lysis/Assay Buffer (100mL).....	31
Table 16: Components of PBS (1L).....	32
Table 17: Reagent Information	34

List of Figures

Figure 1: JPH2 structure and Ca ²⁺ cycling in cardiomyocytes.	5
Figure 2: Mechanisms of JPH2 dysregulation in heart diseases.	9
Figure 3: Palmitate incubation increases caspase-3 activity in neonatal mouse cardiomyocytes.	38
Figure 4: Palmitate incubation increases DNA fragmentation in neonatal mouse cardiomyocytes.	40
Figure 5: Palmitate incubation reduces JPH2 protein expression in neonatal mouse cardiomyocytes.	42
Figure 6: Knockdown of JPH2 with Ad-shJPH2 in neonatal mouse cardiomyocytes.	44
Figure 7: JPH2 knockdown enhances palmitate-induced caspase-3 activity in neonatal mouse cardiomyocytes.	46
Figure 8: JPH2 knockdown enhances palmitate-induced DNA fragmentation in neonatal mouse cardiomyocytes.	48
Figure 9: Over-expression of JPH2 with Ad-JPH2 in neonatal mouse cardiomyocytes.	50
Figure 10: JPH2 over-expression attenuates palmitate-induced caspase-3 activity in neonatal mouse cardiomyocytes.	52
Figure 11: JPH2 over-expression attenuates palmitate-induced DNA fragmentation in neonatal mouse cardiomyocytes.	54
Figure 12: JPH2 knockdown induces caspase-3 activity in neonatal mouse cardiomyocytes.	56
Figure 13: JPH2 knockdown induces DNA fragmentation in neonatal mouse cardiomyocytes.	58

Figure 14: Palmitate incubation increases CHOP protein expression in neonatal mouse cardiomyocytes.	60
Figure 15: JPH2 knockdown increases CHOP protein expression in neonatal mouse cardiomyocytes.	62
Figure 16: JPH2 over-expression attenuates palmitate-induced CHOP protein expression in neonatal mouse cardiomyocytes.	64
Figure 17: CHOP knockout reduces JPH2 knockdown-induced caspase-3 activity in neonatal mouse cardiomyocytes.	66
Figure 18: CHOP knockout reduces palmitate-induced caspase-3 activity in neonatal mouse cardiomyocytes.	68
Figure 19: Inhibition of Ca ²⁺ release from RyR2 reduces palmitate-induced CHOP protein expression in neonatal mouse cardiomyocytes.	70
Figure 20: Inhibition of Ca ²⁺ release from RyR2 reduces JPH2 knockdown-induced CHOP protein expression in neonatal mouse cardiomyocytes.	72
Figure 21: Inhibition of Ca ²⁺ release from RyR2 reduces palmitate-induced caspase-3 activity in neonatal mouse cardiomyocytes.	74
Figure 22 Ryanodine reduces palmitate-induced Ca ²⁺ release in neonatal mouse cardiomyocytes.	76
Figure 23 JPH2 over-expression attenuates palmitate-induced Ca ²⁺ release in neonatal mouse cardiomyocytes.	78
Figure 24: Summary of findings.	84

Chapter 1

1 Introduction

1.1 Cardiac lipotoxicity

Fatty acids (FAs) are the primary lipids used by the heart for energy production. The heart balances uptake, oxidation and metabolism of FAs to maintain ATP production, lipid signaling and membrane biosynthesis (1). Diabetes and obesity are prevalent in western countries. In both conditions, cardiomyocytes take up excessive fatty acids which may alter the structures of cells and activate downstream pathways, leading to cardiomyocyte apoptotic cell death followed by myocardial dysfunction, a condition described as cardiac lipotoxicity (2). This will eventually lead to adverse myocardial remodeling and heart failure (3). However, it remains incompletely understood how the excessive lipids cause cardiac dysfunction and heart failure.

The healthy adult heart acquires 60–80% of its energy requirements by mitochondrial β -oxidation of fatty acids and 20–30% of its energy requirements from glucose. In addition, ketone bodies, lactate and amino acids are also utilized for energy production (4, 5). Normally, the origin of fatty acids supplied to the heart is either plasma fatty acids bound to albumin or fatty acids contained within chylomicron- or very-low density lipoprotein (VLDL)-triacylglycerol (TAG). Free fatty acids are released by lipoprotein lipase (LPL) from chylomicron- or VLDL-TAG and then transported into the cardiomyocytes by diffusion or via protein-mediated uptake. The proteins which mediate free fatty acids uptake involve the cluster of differentiation 36 (CD36), fatty acid transport protein (FATP) and plasma membrane fatty acid binding protein (FABPpm). In the process of protein-mediated fatty acid uptake, the fatty acids are initially bound to FABPpm, and then

transported via FAT/ CD36 or FATP1/6. After transporting into the cytosol, the fatty acids are used for ATP production by mitochondrial β -oxidation, participate in anabolic metabolism into the endogenous TAG pool, or contribute to membrane synthesis through the production of phospholipid (6).

The healthy heart is very flexible in its regulation of overall energy metabolism. However, the balance between energy demand and supply is disturbed under pathological conditions. For example, the increase of fatty acid supply and the subsequent increase of fatty acid uptake induce the lipid accumulation in the heart (7). It is also postulated that mitochondrial dysfunction results in lipid accumulation in the heart by impairing fatty acid β -oxidation (8-10). Excessive lipid accumulation in the heart induces cardiac lipotoxicity which is associated with insulin resistance, cardiomyocyte apoptosis and subsequent cardiac dysfunction (4, 11). As described above, excessive fatty acids accumulated in the cardiomyocytes have several fates. The excessive fatty acids may undergo β -oxidation in the mitochondria for energy metabolism or be stored as TAG (4, 7). However, when the capacity for mitochondrial β -oxidation of fatty acids cannot keep up with the excessive uptake of fatty acids, lipid intermediates will accumulate, including TAG, diacylglycerols (DAGs), ceramides, long-chain acyl CoAs, and acylcarnitines (4, 12, 13). The accumulation of these toxic lipid intermediates may result in mitochondrial dysfunction (14, 15), insulin resistance (16-19), cellular apoptosis (20, 21) and ventricular dysfunction (22-24).

Palmitate (PA) is the most common saturated fatty acid found in western diets (25). According to the World Health Organization, consumption of palmitate increases the risk of developing cardiovascular diseases (26). Palmitate, a saturated fatty acid, has been

widely used in the study of cardiac lipotoxicity. Palmitate-treated neonatal rat cardiomyocytes have elevated reactive oxygen species (ROS) and changes in mitochondrial morphology which are accompanied by the loss of mitochondrial reticulum, suggesting increased mitochondrial fission (27). The level of mitochondrial ROS correlates with mitochondrial dysfunction and apoptosis in cardiomyocytes induced by palmitate (27, 28). Palmitate treatment can also result in down-regulation of peroxisome proliferator-activated receptors (PPARs), which in turn, impair the expression of important proteins involved in mitochondrial β -oxidation (29). Nevertheless, the molecular mechanisms by which palmitate induces mitochondrial dysfunction and cell death have not been fully addressed.

1.2 Junctophilin-2

Junctophilin-2 (JPH2) is encoded by the *JPH2* gene which was discovered about 2 decades ago (30). There are 4 members in the junctophilin protein family (JPH1-4). They bridge the physical gap between the plasma membrane and the sarcoplasmic/endoplasmic reticulum (SR/ER) in excitable cells (31). JPH2 is the main junctophilin isoform in the heart, although JPH1 is also expressed to a lesser extent (30). JPH1 is the major isoform in skeletal muscle and JPH3 and JPH4 are neuronal isoforms found in brain (32).

Junctophilins are highly conserved molecules. There are 4 different components of JPH2 (33) (Figure 1). The 8 ‘membrane occupation and recognition nexus’ (MORN) motifs (~330 amino acids) in the N-terminal region are thought to mediate attachment to the plasma membrane. The MORN motif region is followed by a well-conserved α -helical domain (~100 amino acids) which serves as the structural basis for the maintenance of a uniform distance between the plasma membrane and the SR/ER. There is also a putative

divergent region which exhibits a high degree of conservation (83%–91%) across species, but shows poor conservation across the 4 JPH isoforms (15%–17%). The function of this domain is not clear presently, but it may be associated with isoform-specific JPH functions. Finally, JPH2 binds to the ER/SR membrane by a C-terminal, 22-amino acid transmembrane anchor (30).

JPH2 is a membrane-binding protein that maintains a fixed distance between the plasma membrane and the SR/ER, which plays an important role for proper Ca^{2+} -induced Ca^{2+} release during the excitation-contraction process (31). Also, JPH2 is essential for the development of postnatal T-tubules in mammals (34, 35). It can also maintain the architecture of the junctional membrane complexes (JMCs) and stabilize local ion channels in mature cardiomyocytes (36). A recent study also shows that JPH2 can stabilize the activity of ryanodine receptor 2 (RyR2) in cardiomyocytes (36). Interestingly, it is recently found that JPH2 can be cleaved by the Ca^{2+} dependent protease, calpain under stress and the liberated N-terminal fragment of JPH2 (JP2NT) can serve as a transcription regulator, inducing cardioprotective transcriptional reprogramming (37). All of these prior findings underscore an important role of JPH2 in cardiac pathophysiology. In line with this, JPH2 dysfunction of mutations or down-regulation has been associated with hypertrophic cardiomyopathy, arrhythmias, and heart failure (35).

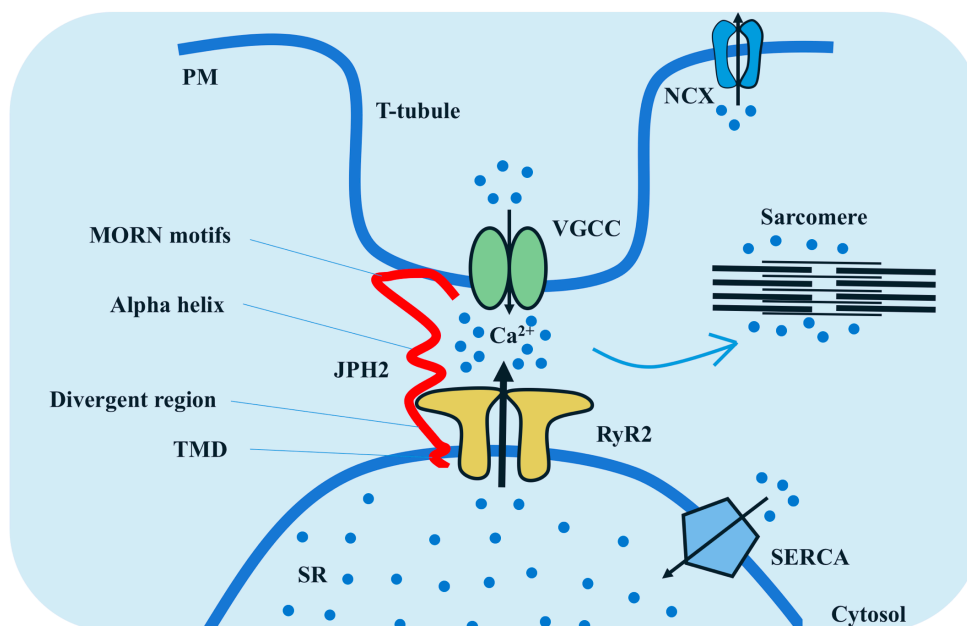


Figure 1: JPH2 structure and Ca^{2+} cycling in cardiomyocytes.

JPH2 is composed of the N-terminal MORN motifs, alpha helix region, divergent region and transmembrane domain. In cardiomyocytes, the entry of a small amount of Ca^{2+} via VGCC triggers the opening of RyR2 and the release of a large amount of Ca^{2+} from the SR, a process described as Ca^{2+} -induced Ca^{2+} release or Ca^{2+} coupling. The ensuing increase of cytoplasmic Ca^{2+} enables contraction. Finally, Ca^{2+} is removed from the cytoplasm back into the SR by SERCA pump and out of the cell by NCX. JPH2: junctophilin-2; VGCC: voltage-gated Ca^{2+} channel; RyR2: ryanodine receptor-2; SERCA: sarco/endoplasmic reticulum Ca^{2+} ATPase pump; NCX: $\text{Na}^+/\text{Ca}^{2+}$ exchanger; PM: plasma membrane; SR: sarcoplasmic reticulum; MORN: membrane occupation and recognition nexus; TMD: transmembrane domain.

1.2.1 JPH2 in T-tubule maturation

Knockdown of JPH2 by cardiac-specific short hairpin RNA (shRNA) in mice destroys the formation of mature T-tubules within the first few weeks of life (35). Conversely, the maturation of T-tubules occurs earlier in mice over-expressing JPH2 (35). This study suggests that JPH2 is highly involved in the development of T-tubules to induce membrane invagination. T-tubule architecture has been reported to be pathologically remodeled in both patients and animal models with failing hearts (38). A high rate of mortality with rapid development of systolic heart failure is found in mice with acute conditional cardiac

shRNA-mediated knockdown of JPH2 (39). Similarly, JPH2 expression is decreased in the myocardial ischemia model with loss of colocalization of JPH2 and RyR2 (40). While the loss of JPH2 has yet to be studied in patients with more diverse cardiac disease etiologies, the disruption of T-tubule architecture which occurs in ischemic heart disease, idiopathic dilated cardiomyopathy, and hypertrophic cardiomyopathy (HCM) is likely a very early event in failing hearts (34, 41, 42).

1.2.2 JPH2 in the postnatal development of junctional membrane complexes (JMCs)

JPH2 can anchor T-tubules and SR. JPH2 null mice are embryonically lethal by Day E10.5 when the heart normally initiates contractile function, demonstrating the important function of JPH2 (30). There is an extensive loss of JMCs in the JPH2 null mice in association with spontaneous SR Ca^{2+} release and irregular Ca^{2+} transients, indicating that JPH2 is very important in the postnatal development of JMCs (36). Cardiac-specific JPH2 knockdown reduces the number of JMCs, increases the variability of the distance between the plasma membrane and the SR/ER and results in impaired cardiac contractility, leading to heart failure and increased mortality (39). JPH2 deficiency affects T-tubule elements preferentially, suggesting that longitudinal tubule elements may be JPH2 independent, which is correlated with changes in T-tubule structure and JPH2 down-regulation in heart failure (43).

1.2.3 JPH2-mediated regulation of RyR2

While the importance of JPH2 for T-tubule function has received significant attention, T-tubule independent functions of JPH2 in cardiomyocytes have just been recognized. Decreased or dysfunctional JPH2 results in RyR2 dysfunction in cardiomyocytes,

indicating a novel role of JPH2 in maintaining RyR2 stability, which is independent of the T-tubule system (35). Studies using mice with a JPH2 missense mutation (JPH2-E169K) reveal that dysfunctional JPH2 disrupts the interaction between RyR2 and JPH2 and thus leads to Ca^{2+} leak from RyR2 (37, 44). This results in an increase in diastolic Ca^{2+} and promotes the activation of sarcolemmal Na^+ - Ca^{2+} exchanger (NCX), thereby creating a net depolarizing current, leading to delayed afterdepolarizations (DADs), an important mechanism contributing to atrial arrhythmias (45-47). Therefore, arrhythmogenic SR Ca^{2+} leak may be initiated by the loss of the stabilizing interaction between JPH2 and RyR2. However, the molecular mechanisms by which JPH2 stabilizes RyR2 remain unknown. Given the importance of Ca^{2+} cycling in cardiac bio-pathology, this novel function of JPH2 may be important in maintaining cardiac normality, suggesting that a reduction and/or dysfunction of JPH2 may play a role in cardiac injury under stress.

1.2.4 Regulation of JPH2 in cardiomyocytes

JPH2 down-regulation has been involved in various cardiac diseases and some mechanisms have been suggested to explain the loss of JPH2 (Figure 2). It is shown that JPH2 is the target of microRNA 24 (miR-24), which may be responsible for decreased JPH2 in cardiac hypertrophy (48). In failing hearts, miR-24 is up-regulated (48, 49), and is associated with the down-regulation of JPH2 (48, 50). Silencing miR-24 prevents the development of heart failure which is said to be due to maintaining the expression of JPH2 and T-tubule integrity (51), confirming the relationship between miR-24 and JPH2. Another study finds that JPH2 is the target of miR-34a. Initial cardiac defects diminish RBFox2 (RNA binding protein) expression, which induces the expression of miR-34a, and elevated miR-34a targets JPH2 to down-regulate JPH2 expression, which further results in heart dysfunction, leading to

progressive heart failure. The administration of a miR-34a mimic is sufficient to induce cardiac defects. However, antagonism of miR-34a alleviates RBFOX2 depletion-induced heart dysfunction (52).

JPH2 down-regulation has also been attributed to cleavage by calpain in failing hearts (53). Calpain is a protease that is activated by elevated intracellular Ca^{2+} (54, 55). Activation of the heterotrimeric G protein $G_{\alpha q}$ can activate calpain. Loss of T-tubule integrity, together with a pronounced decrease in full-length JPH2 are found in a transgenic mouse with inducible activation of the heterotrimeric G protein $G_{\alpha q}$. Calpain inhibitors prevent $G_{\alpha q}$ -mediated JPH2 down-regulation, suggesting calpain is responsible for generation of the JPH2 cleavage fragments (53). Furthermore, decreased full-length JPH2 level is found in ischemia-reperfusion injury, though no cleavage fragment is detected (56).

A most recent study shows that JPH2 is also a target of matrix metalloproteinase-2 (MMP2) in myocardial ischemia-reperfusion (IR) injury (57). MMP2 is a Zn^{2+} and Ca^{2+} -dependent protease that is activated by oxidative stress in myocardial IR injury which cleaves both intracellular and extracellular substrates. IR injury increases the degradation of JPH2 and impairs the recovery of cardiac contractile function. ARP 100, a MMP inhibitor, attenuates JPH2 proteolysis and improves the recovery of cardiac contractile function in IR hearts. In addition, MMP2 is co-localized with JPH2 in IR hearts. It is confirmed that JPH2 is susceptible to proteolysis by MMP2 and multiple cleavage sites have been predicted (57). In addition to its down-regulation, loss of normal subcellular localization of JPH2 due to microtubule polymerization also contributes to JPH2 dysregulation (58). Microtubule densification, defined as the increase in microtubule density due to enhanced microtubule polymerization, is commonly found in human failing hearts and mouse models of heart

failure (56, 59). Zhang et al. observed that the subcellular distribution of JPH2 is linked to microtubule dynamics (58). Under cardiac stress, redistribution of JPH2, resulting from the densification of the microtubule network, induces T-tubule remodeling and excitation-contraction coupling dysfunction, contributing to the development of heart failure (58).

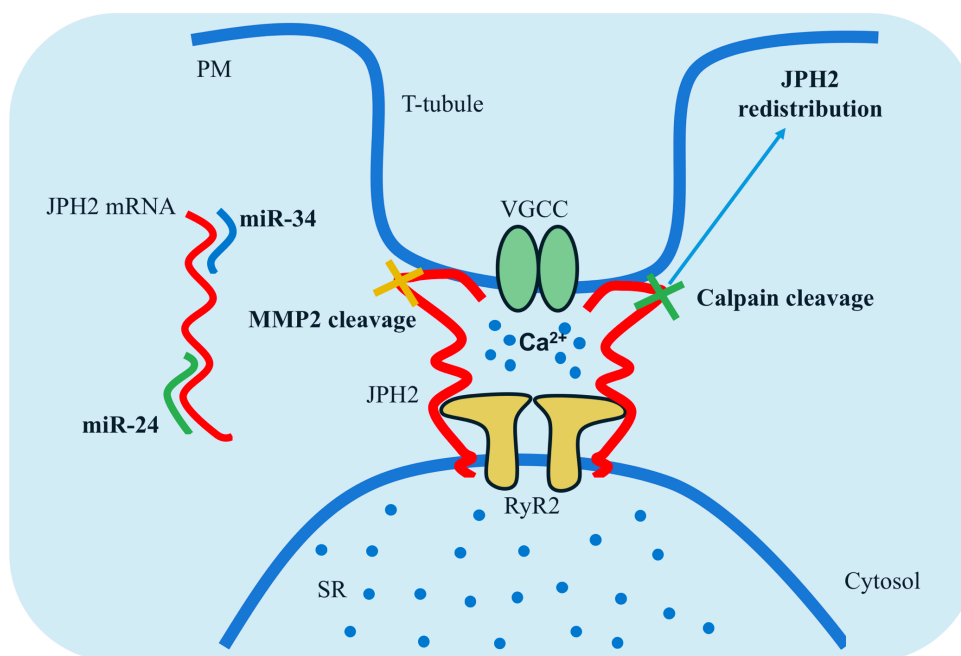


Figure 2: Mechanisms of JPH2 dysregulation in heart diseases.

Depicted are miRNA-mediated gene silencing by miR-24 and miR-34, calpain-mediated proteolysis, MMP2-mediated proteolysis, and redistribution to the cell periphery in response to microtubule polymerization. JPH2: junctophilin-2; VGCC: voltage-gated Ca^{2+} channel; RyR2: ryanodine receptor-2; miR: micro RNA; MMP2: matrix metalloproteinase-2; PM: plasma membrane; SR: sarcoplasmic reticulum.

1.2.5 JPH2 encodes transcription regulator under stress

JPH2 is required for normal E-C coupling. After cardiac stress, Ca^{2+} overload induces protease calpain activation. JPH2 is cleaved by calpain and liberates the N-terminal fragment (JP2NT), disrupting the ultrastructure of the E-C coupling machinery. JP2NT translocates to the nucleus via a conserved nuclear localization signal, binds to the TATA box of genomic DNA via the alanine-rich region and associates with a MEF2 response

element to repress the transcription of genes that control deleterious cardiac remodeling (37). Transgenic over-expression of JP2NT in mice results in attenuated pathological remodeling in response to cardiac stress. Conversely, loss of nuclear JP2NT function accelerates stress-induced development of hypertrophy and heart failure in mutant mice (37). This finding reveals that cardiomyocytes possess a self-protective mechanism in failing cardiomyocytes that transduces mechanical information (E-C uncoupling) into transcriptional reprogramming in the stressed heart (37).

1.3 Endoplasmic reticulum stress

The endoplasmic reticulum (ER) is a multifunctional intracellular organelle supporting many processes required by almost every mammalian cell, including cardiomyocytes. It performs diverse functions, including protein synthesis, translocation across the membrane, integration into the membrane, folding and posttranslational modification (60). Also, the ER participates in the synthesis of phospholipids and steroids on the cytoplasmic side of the ER membrane (61). It is also the major intracellular Ca^{2+} reservoir in the cell and plays an important role in the regulation of Ca^{2+} homeostasis in cardiomyocytes (62, 63).

ER stress is a condition that is accelerated by the accumulation of unfolded/misfolded proteins after the disturbance in ER quality control in a variety of physiological and pathological conditions (64). Upon ER stress, cells activate a series of complementary adaptive mechanisms to cope with protein-folding alterations, which together are known as the unfolded protein response (UPR) (63). The UPR transduces information about the protein-folding status in the ER lumen to the nucleus and cytosol to buffer fluctuations in unfolded/misfolded protein load (65, 66). When cells undergo irreversible ER stress, this pathway eliminates damaged cells by apoptosis (67). ER stress is found to be involved in

many cardiovascular diseases, such as ischemic heart disease, atherosclerosis, cardiac hypertrophy, cardiac lipotoxicity, heart failure etc. (68).

1.3.1 Unfolded protein response (UPR)

UPR is a defense mechanism which removes the unfolded/misfolded proteins and prevents their accumulation. The UPR is activated by 3 main transmembrane stress sensors, including inositol-requiring protein 1 α (IRE1 α), protein kinase RNA-like ER kinase (PERK) and activating transcription factor 6 (ATF6) and results in a lot of cellular responses (63, 68).

In the IRE1 α pathway, IRE1 α dimerization triggers the activation of its RNase, which promotes the mRNA encoding unspliced X box-binding protein 1 (XBP1) and produces a transcription factor, spliced XBP1 (XBP1s). XBP1s regulates the transcription of genes which encode proteins involved in protein folding, protein quality control, phospholipid synthesis and ER-associated degradation (ERAD). IRE1 α can degrade some mRNAs through regulated IRE1-dependent decay (RIDD). IRE1 α can also trigger 'alarm stress pathways', including those driven by nuclear factor- κ B (NF- κ B) and JUN N-terminal kinase (JNK) (63, 69).

In the PERK pathway, PERK activation can phosphorylate the initiation factor eukaryotic translation initiator factor 2 α (eIF2 α) to prevent the synthesis of general protein. PERK activation can also phosphorylate the nuclear factor erythroid 2-related factor 2 (NRF2) which is a transcription factor controlling redox metabolism. eIF2 α phosphorylation allows the translation of the transcription factor ATF4, which regulates the transcription of genes participating in apoptosis, autophagy, antioxidant responses and amino acid metabolism. (63, 70).

In the ATF6 pathway, there is a basic Leu zipper (bZIP) transcription factor in the cytosolic domain of ATF6 and it is localized to the ER. When cells undergo ER stress, ATF6 can be transported to the Golgi apparatus by interacting with the coat protein II (COPII) complex. Then, ATF6 is processed by site 1 protease (S1P) and S2P and its cytosolic domain fragment (ATF6f) is released. ATF6f regulates the up-regulation of genes encoding XBP1 and ERAD components (63, 71).

These 3 branches of ER transmembrane sensors can trigger adaptive responses through the splicing of XBP1, the phosphorylation of eIF2 α and the translation of transcription factor ATF4. Finally, the unfolded protein response related genes are induced, including CCAAT-enhancer-binding protein (C/EBP) homologous protein (CHOP), chaperones glucose-regulated protein-78 (GRP78), GRP94 etc (2).

1.3.2 Calcium homeostasis and ER stress

As described above, ER stress is induced by the accumulation of unfolded/misfolded proteins. It is shown that oxidative stress, ischemia, disturbance of Ca²⁺ homeostasis and high-fat diet are related to the induction of ER stress (2, 72-74).

In cardiomyocytes, sarcoplasmic/endoplasmic reticulum (SR/ER) is the major intracellular Ca²⁺ reservoir. The entry of a small amount of Ca²⁺ through L-type Ca²⁺ channels on plasma membrane during an action potential triggers the synchronized opening of RyR2 on the SR which allows a rapid and transient release of Ca²⁺ from the SR. This process is described as Ca²⁺-induced Ca²⁺ release (CICR) or Ca²⁺ coupling. The subsequent elevation of intracellular Ca²⁺ promotes the contraction of cardiomyocytes. Finally, Ca²⁺ is removed from the cytoplasm back into the SR by sarcoplasmic/endoplasmic reticulum ATPase (SERCA2a) pump and out of the cell by Na⁺-Ca²⁺ exchanger (NCX) (Figure 1) (75).

Ca²⁺ homeostasis refers to the regulation of Ca²⁺ concentration in the body. This concentration is tightly controlled by a stabilizing system consisting of Ca²⁺ channels and Ca²⁺ buffering proteins (76). Ca²⁺ homeostasis is crucial for cell survival. The disruption of Ca²⁺ homeostasis induces ER stress and leads to the apoptotic cell death (76). Reticulocalbin 1 (RCN1), a target of NF-κB, suppresses ER Ca²⁺ release by binding to inositol 1,4,5-trisphosphate receptor type 1 (IP3R1) and decreases the UPR, thereby inhibiting ER stress-induced apoptosis (77). The Ca²⁺ channel RyRs are involved in ER stress and β-cell death (78). In this study, ER stress following SERCA inhibition is attenuated by blocking RyRs. Conversely, stimulation of RyRs accelerates thapsigargin-induced ER depletion and apoptosis (78).

1.3.3 ER stress and apoptosis

If ER stress is prolonged or overwhelming, it can induce apoptotic cell death through CHOP and/or other pathways (79).

CHOP, also known as growth arrest- and DNA damage-inducible gene 153 (GADD153), is a 29 kDa protein with 169 (human) or 168 (rodents) amino-acid residues. It is composed of 2 known functional domains, an N-terminal transcriptional activation domain and a C-terminal basic-leucine zipper (bZIP) domain (80). CHOP is ubiquitously expressed at very low levels and is present in the cytosol under nonstressed conditions. However, ER stress can induce the expression of CHOP and lead to its accumulation in the nucleus (81). CHOP works as a transcription factor that regulates genes involved in apoptotic cell death (82, 83).

CHOP is the main up-regulated pro-apoptotic player during excessive ER stress (84). The transcriptional induction of CHOP is controlled by the PERK–ATF4 axis in a positive

manner (79) and this up-regulation switches the consequences of the UPR from proadaptive to proapoptotic signaling. In addition to the inhibition of Bcl-2, over-expression of CHOP promotes several mechanisms of apoptosis including the stimulation of caspase activity (85) and Bax translocation from cytosol to mitochondria (86). Knockdown of CHOP reduces ER stress-mediated apoptosis (82) and over-expression of CHOP triggers apoptosis after treatment with ER stress inducers (85).

1.3.4 ER stress in cardiovascular diseases

Recent animal and human studies have demonstrated that ER stress is implicated in the pathophysiology of various cardiovascular diseases (83, 87). In ischemic heart disease, cell death is reduced in cardiomyocytes after the inhibition of ER stress and silencing of the IRE1 gene (88). In addition, the ER may induce apoptotic signaling by increasing the expression of CHOP involved in the transition from cardiac hypertrophy to heart failure (83). In atherosclerosis, the intensity of ER stress increases and the PERK pathway induces cell death by activating IRE1 α and inducing apoptosis signaling pathways (87).

Notably, ER stress is induced and has been implicated in cardiac lipotoxicity. Our previous work found that in high fat diet fed mouse hearts, ER stress was induced and apoptosis was increased. In addition, palmitate also induced ER stress and apoptotic cell death compared to oleate in cultured cardiomyocytes (2). These results mean that ER stress is induced and detrimental under cardiac lipotoxicity condition. However, sequestration of fatty acids in triglycerides can prevent ER stress in an in vitro model of cardiomyocyte lipotoxicity (89).

1.4 Apoptosis in cardiomyocytes

1.4.1 Apoptosis: programmed cell death

Apoptosis is widely known as programmed cell death which may occur in multicellular organisms. Apoptosis can result in characteristic cell changes and death. There are 3 classic signaling pathways of apoptosis, including the intrinsic (mitochondrial) pathway, the extrinsic (death receptor) pathway, and the ER stress pathway.

1.4.1.1 The morphological change of apoptosis

Apoptosis is an organized self-killing process (90). The cells begin to shrink after the activation of apoptotic pathways. Morphological changes include smaller cellular size, denser cytosol, chromatin condensation and more tightly packed organelles. Subsequently, apoptotic bodies are formed, where the plasma membrane encloses the tightly packed organelles with or without a nuclear fragment. At the same time, nuclear proteins and cytoskeletal proteins are cleaved and degraded by caspases in the execution phase of apoptosis (91). Finally, macrophages will phagocytose the apoptotic bodies through binding to the externalized phosphatidylserine, which is located on the outer leaflet of the bilayer (92).

Many cellular killing and engulfment proteins are involved in the apoptotic process, among which caspases play very important roles. Once the apoptotic pathways are initiated, the activated caspases will activate other procaspases, promoting the protease cascade and then amplifying the apoptotic signal irreversibly (93). Recently, more than 10 caspases have been found and recognized during the apoptotic process, including the initiators (caspase-2,-8,-9,-10), the executioners (caspase-3,-6,-7) and other regulators (caspase-11,-12,-13,-14) (91, 94).

1.4.1.2 The extrinsic pathway

The extrinsic pathway is triggered by transmembrane death receptors which belong to tumor necrosis factor (TNF) receptor family and contain a death domain. Several classical ligands and their corresponding death receptors are apoptosis-stimulating fragment ligand (FasL)/FasR, and TNF- α /TNFR1. TNF-related apoptosis-inducing ligand (TRAIL)/DR4 and TRAIL/DR5 will transmit the death signals from cell surface to intracellular pathways through the death domain. For example, after the binding of FasL to FasR or TNF- α to TNFR1, the fas-associated death domain (FADD) will be recruited and bound to the ligand-receptor complex (95). Subsequently, FADD will activate procaspase-8 and form a death-inducing signaling complex (DISC) (96). Finally, caspase-8 activated by DISC will trigger the activation of caspase-3 and caspase-7 and then induce the apoptotic cascade, leading to the execution phase of apoptosis (97).

1.4.1.3 The intrinsic pathway

The intrinsic pathway is mitochondrial-triggered. This pathway is usually activated by stimuli including hypoxia, hyperthermia and the absence of growth factors. These stimuli promote the opening of mitochondrial permeability transition pore (MPTP) and then accelerate the release of some pro-apoptotic proteins including cytochrome c (Cyt c) and apoptosis-inducing factor (AIF) from the mitochondrial intermembrane space into the cytosol (98). Cyt c will bind and activate apoptotic protease activating factor 1 (Apaf-1) as well as procaspase-9 and then result in the activation of caspase-9, which in turn activates caspase-3 and caspase-7 (99, 100). However, AIF will translocate to the nucleus and induce chromatin condensation and DNA fragmentation in a caspase-independent way in the late phase of apoptosis (101).

Notably, intrinsic pathway-induced apoptosis is regulated by B-cell lymphoma 2 (Bcl-2) family proteins (102) which are in the outer membrane of mitochondria. Bcl-2 family proteins can control the permeability of mitochondrial membrane and participate in the regulation of the release of Cyt c. Bcl-2 family proteins can be classified into pro-apoptotic and anti-apoptotic proteins. The pro-apoptotic proteins include Bax, Bad, Bak, Bim, Bid, Puma and BNIP3 (103); while the anti-apoptotic proteins contain Bcl-2, Bcl-XL, Bcl-x, and BAG (104). Bax can be up-regulated by the tumor suppressor protein p53 in the nucleus or mitochondria (np53 or mp53) (100, 105). However, Bcl-2 or Bcl-xL may block np53 or mp53-induced apoptosis (104-106). When p53 is down-regulated, Bax and caspase-3 are also down-regulated in the heart (107). Interestingly, there is interaction between the extrinsic and intrinsic pathways. It is found that Fas-mediated apoptosis can also induce mitochondrial damage through the caspase-8-mediated cleavage of Bid (108).

1.4.1.4 The ER stress pathway

The ER stress pathway is a relatively newly described pathway contributing to the regulation of apoptosis. It is commonly induced under some physiological or pathological conditions including protein folding, disruption of intracellular Ca^{2+} homeostasis, hypoxia, oxidative stress, ischemia and lipid metabolic disorders (65, 109). Although ER stress is important for cell survival (65), it can also result in apoptosis under prolonged or chronic stimulation (110). As described before, ER stress is sensed by UPR which is activated by 3 main stress sensors including IRE1 α , PERK and ATF6 (62).

In the IRE1 α pathway, IRE1 α interacts with TRAF2 (tumor necrosis factor receptor (TNFR)-associated factor-2) and initiates JNK expression which is demonstrated to be involved in cell death (111, 112). Therefore, it is assumed that JNK is associated with IRE1-

mediated apoptosis. Notably, IRE1 α can be activated through binding to Bak and Bax (113). Procaspase-12 is activated through interacting with IRE1 α -TRAF2 complex (114). In addition, IRE1 α may promote apoptosis by activating the RIDD pathway (79, 115); however, the specific mechanism is unclear. Interestingly, IRE1 α can also splice and activate XBP1 mRNA (116) which participates in cell survival. As a result, IRE1 α is a crucial protein and plays an important role in the regulation of apoptosis and survival under ER stress.

In the PERK pathway, PERK promotes the phosphorylation of eIF2 α and induces the translation of ATF4, which participates in proapoptotic process. ATF4 induces the expression of CHOP. CHOP can suppress the expression of Bcl-2 (85) and increase the expression of Bim, Puma and Bax (117-120). Also, CHOP can activate ER oxidase 1 α (ERO1 α) (121) and induce Ca²⁺-dependent apoptosis through the CHOP-ERO1 α -IP3R1-Ca²⁺-CaMKII pathway (122). Caspase-12 and Bid are also reported to be involved in CHOP-ERO1 α -IP3R- Ca²⁺-calpain pathway during ER stress (123, 124). Notably, CHOP- and IRE1 α -induced apoptosis can be repressed by a phenomenon called pre-conditioning, where low-level ER stress can partially prevent UPR before a robust UPR activation (125). In the ATF6 pathway, ATF6 can activate XBP1 and exert a prosurvival effect (116). Conversely, inhibition of ATF6 can promote apoptosis (126). However, the detailed mechanism of ATF6-involved apoptosis needs further investigation.

1.4.2 Apoptosis in cardiac lipotoxicity

1.4.2.1 Cardiac lipid overload induces apoptosis

Cardiac lipid overload is associated with, and thought to contribute to, the initiation of the apoptotic cascade. Studies, primarily in isolated cardiomyocytes, have implicated saturated

FAs as a primary cause of apoptosis (127). Treatment of isolated neonatal rat ventricular myocytes with palmitic acid can generate cytoplasmic ceramide, which activates JNK1/2 that interacts with Bax in the mitochondrial membrane, leading to apoptosis associated with cardiolipin loss, cytochrome c release, mitochondrial swelling, and DNA laddering (127, 128).

Accumulation of FAs has been linked to the induction of ER stress. Specifically, palmitate-induced ER stress has been considered to be a secondary event that follows oxidative stress and the generation of ROS, and results in an induction of eukaryotic elongation factor (eEF) 1A-1, which interferes with the integrity of the cytoskeleton and causes cell death (129). A more direct mechanism of palmitate-induced ER stress has also been proposed in the same study. This mechanism involves the incorporation of palmitate in phospholipid and TG species in microsomal membranes so that ER membrane integrity is compromised and protein-folding chaperones are redistributed to the cytosol (130). Another study has reported that the esterification of palmitate can directly cause ER fission (131). Intensive ER stress may result in apoptosis.

1.4.2.2 Apoptosis induces cardiomyocyte dysfunction and cardiac remodeling

Cardiac lipid overload is associated with, and thought to contribute to, the initiation of the apoptotic cascade. Cardiomyocyte loss via apoptosis together with pathological cardiomyocyte hypertrophy may produce progressive myocardial dysfunction, leading to heart failure (132). Cardiac hypertrophy occurs in response to long-term increases in hemodynamic load related to various physiological and pathological conditions. The hypertrophic process is characterized by structural changes at the cardiomyocyte level that

are translated into alterations in chamber size and geometry, collectively called remodeling (133, 134). Functional benefits of the hypertrophic response include an increase in the number of contractile elements, a lowering of wall stress through increased wall thickness in concentric hypertrophy, and an increase of stroke volume by increasing end-diastolic volume in eccentric hypertrophy (134). By contrast, pathological forms of cardiac hypertrophy develop in response to persistent increases in hemodynamic load. Epidemiological studies have demonstrated that pathological cardiac hypertrophy is a risk factor for future cardiac events (135, 136). Indeed, pathological cardiac hypertrophy often enters a phase of pathological remodeling that leads to contractile dysfunction, heart failure and sudden death (137).

Cardiomyocyte loss via apoptosis also participates in cardiac fibrosis (138). Fibrosis is the excessive deposition of extracellular matrix (ECM), such as collagens and fibronectin, resulting in the excessive accumulation of fibrous connective tissue (139, 140). Fibrosis is an essential process in the repair of damaged tissues and wounds, but its accumulation in organs and tissues can lead to scarring, organ dysfunction and, ultimately, failure (138). Paracrine signaling from fibroblasts induces cardiomyocyte hypertrophy. Fibroblasts can produce a number of cytokines and growth factors, including TGF- β , interleukin-33 (IL-33), fibroblast growth factor 2 (FGF2), tumor necrosis factor alpha (TNF- α), insulin growth factor (IGF1) and endothelin-1 (ET-1), which directly affect cardiomyocyte function in vitro and/or in vivo (141-148). Myofibroblasts express a large number of structural ECM proteins and matrix remodeling proteins and together determine the functionality of the ECM. Thus, besides the amount of ECM, the level of collagen cross-linking also strongly determines the development of diastolic and systolic dysfunction (137, 149-154). Fibrosis

also disturbs cardiac electrophysiology and induces rhythm disturbances. In mice, TGF- β over-expression results in atrial fibrosis, without ventricular involvement, and these mice develop inducible atrial fibrillation (AF) (155, 156). Finally, fibrosis limits nutrient supply to the myocardium by limiting cardiac function and myocardial blood flow (149). Perivascular fibrosis in coronary arteries reduces oxygen delivery toward myocardial tissue, reduces coronary reserves and promotes myocardial ischemia (137, 154). Thus, fibrosis impairs cardiac function by at least 3 mechanisms, including induction of myocardial stiffness, induction of atrial fibrillation and limiting oxygen and nutrient supply to the stressed myocardium. These will promote cardiomyocyte hypertrophy and heart failure.

1.5 Rationale

Cardiac lipotoxicity is a critical mechanism underlying cardiac complications in patients with obesity and/or diabetes. Cardiac lipotoxicity results from the accumulation of lipid intermediates in non-adipose tissue, leading to cellular dysfunction and death. However, it needs to be further elucidated how the accumulation of lipids causes cellular dysfunction and death in the heart.

In our lab, we previously reported that palmitate treatment activated calpain and induced ER stress and subsequent cell injury when compared to oleate in cardiomyocytes (2). We further found that the protein levels of JPH2 were reduced in high fat diet-fed mouse hearts, which correlated with myocardial injury and dysfunction (2). These previous findings raise an important possibility that decreased JPH2 may play a role in mediating ER stress and apoptosis in cardiomyocytes during lipotoxicity and thus, up-regulation of JPH2 may protect cardiomyocytes against lipotoxicity.

Understanding the role of JPH2 in cardiac lipotoxicity is clinically relevant because the protein levels of JPH2 are reduced in various human diseased hearts. This study determines whether and how JPH2 provides a cardiac protective role in lipotoxicity.

1.6 Hypothesis

JPH2 will protect cardiomyocytes against palmitate-induced injury by inhibiting endoplasmic reticulum (ER) stress.

1.7 Specific aims

1.7.1 To confirm that palmitate induces cell injury in cardiomyocytes.

1.7.2 To determine if JPH2 knockdown enhances whereas JPH2 over-expression attenuates palmitate-induced cell injury in cardiomyocytes.

1.7.3 To determine the mechanism by which JPH2 protects cardiomyocytes against palmitate-induced injury by modulating calcium release from RyR2 and inhibiting ER stress.

Chapter 2

2 Materials and Methods

2.1 Animals

This investigation conforms to the Guide for the Care and Use of Laboratory Animals published by the US National Institutes of Health (NIH Publication, 8th Edition, 2011). All experimental procedures were approved by the Animal Use Subcommittee at the University of Western, Ontario, Canada. Breeding pairs of C57BL/6 mice and C57BL/6 background CHOP^{-/-} mice were purchased from the Jackson Laboratory (Bar Harbor, Maine). Mice used in this study, including controls, were littermates.

For genotyping of CHOP^{-/-} mice, 1-2 mm of the tip of the tail was cut from CHOP^{-/-} mice and put into a microtube (1.5mL). The DNA from CHOP^{-/-} mice was extracted. Briefly, the tail was lysed in solution A (Table 1) and incubated in a metal bath at 100 °C for 45 min. Then, the microtube containing solution A was cooled to room temperature. The stabilization buffer solution B (Table 2) was added to the microtube and mixed completely. After that, the DNA lysate was centrifuged at 10,000g for 5 min and the supernatant was ready for PCR (FroggaBio). The PCR system (Table 3) and protocol (Table 4) for the gene amplifying of CHOP are listed below. It was confirmed that there was no CHOP gene expression in CHOP^{-/-} mice.

Table 1: Components of Solution A (100mL)

NaOH	100 mg
EDTA	7.4 mg
H ₂ O	100 mL

Table 2: Components of Solution B (100mL)

Tris-HCl (40mM, pH=5.0)	0.48 g
H ₂ O	100 mL

Table 3: Components of PCR System (25 μ L)

10X Buffer	2.5 μ L
2.5 mM dNTP	2 μ L
Taq DNA polymerase (5U/ μ L)	0.25 μ L
25uM Primer	0.4 μ L
H ₂ O	17.85 μ L
Template DNA	2 μ L

Table 4: Protocol of PCR for CHOP^{-/-} Mouse

Step	Temperature ($^{\circ}$ C)	Time
1	94	2 min
2	94	20 sec
3	65 (- 0.5 $^{\circ}$ C per cycle decrease)	15 sec
4	68	10 sec
5	Repeat step 2-4 for 10 cycles	
6	94	15 sec
7	60	15 sec
8	72	10 sec
9	Repeat step 6-8 for 30 cycles	
10	72	2 min
11	10	∞

2.2 Isolation and culture of neonatal mouse cardiomyocytes

Primary cardiomyocytes were isolated from neonatal mice born within 24 hours. Briefly, after sterilizing with 75% alcohol, the neonatal mice were killed by decapitation. The chest was opened through a sternal approach and the hearts were harvested and placed into D-Hank's solution (50 mL tube, Table 5). The hearts were washed in D-Hank's solution 2 times to remove the blood. Then, each heart was cut into 5–6 pieces by a surgical blade

and washed in D-Hank's solution for the third time. The heart pieces were then subjected to the following 3 steps of digestion. (1) Heart tissues were incubated with Liberase Blendzyme (2.5 mg/mL, Roche Applied Science) which was dissolved in sterile water in a water bath at 37°C for 10 min. The supernatant was discarded. (2) The tissues were incubated with fresh Liberase Blendzyme solution at 37°C for 15 min. During the incubation, the heart pieces were gently shaken every 5 min. After 15 min, the heart pieces were triturated to isolate the cardiomyocytes completely. The supernatant containing isolated cardiomyocytes was collected and the culture medium DMEM containing 10% NBCS (new-born calf serum) (Wisent Inc) was added to stop the digestion. (3) Step 2 described above was repeated. The supernatants from steps 2 and 3 were pooled and centrifuged at 200 g for 5 min. The pellets containing the isolated cardiomyocytes were re-suspended in 10% NBCS DMEM. Next, the suspended cells were seeded in a culture dish which was placed in a CO₂ incubator at 37°C for 120 min. This step allowed the fibroblasts to adhere to the culture plate. After fibroblast adherence, cardiomyocytes were collected and the cell number was counted. The cardiomyocytes were then seeded into a culture plate which had been already plated with 1% gelatin (Sigma) at 37°C for 120 min in an incubator. Finally, the plate containing cardiomyocytes was placed in a CO₂ incubator at 37°C. After overnight incubation, the cardiomyocytes were ready for various experiments. The neonatal cardiomyocytes were characterized by the staining of troponin and the purity level was more than 95%.

Table 5: Components of D-Hanks (1L)

KCl	0.4 g
KH ₂ PO ₄	0.06 g
NaCl	8 g
D-Glucose	1 g
Phenol red	0.012 g

2.3 Adenoviral infection

Primary neonatal mouse cardiomyocytes were infected with recombinant adenoviral vectors expressing junctophilin-2 (Ad-JPH2), shRNA for junctophilin-2 (Ad-shJPH2), green fluorescent protein (Ad-GFP) or human influenza hemagglutinin (aa98-106) peptide tag (Ad-HA). The adenoviral vectors were purchased from Vector Biolabs or SignaGen Laboratories. The shRNA sequence of junctophilin-2 (Ad-shJPH2, mouse) is CCTACATGGGCGAGTGGAA-TTCAAGAGA-TTCCACTCGCCCATGTAGG-TTTTTT and the Genbank RefSeq is NM_021566. The titer of the recombinant adenovirus was calculated based on its cytopathic effect (CPE) and the neonatal cardiomyocytes were infected at a multiplicity of infection (MOI) of 100 plaque forming units per cell (100 PFU/cell). The day before the infection, neonatal cardiomyocytes were seeded in a 24-well plate. The adenoviruses were thawed on ice, prepared in 10% NBCS DMEM and added to the cardiomyocytes. After incubation for 4 hours at standard cell culture condition, the cardiomyocytes were supplied with fresh culture medium. Neonatal cardiomyocytes were collected for the following experiments. All the experiments were completed within 72 hours after adenoviral infection.

2.4 Sodium dodecyl sulphate-polyacrylamide gel electrophoresis (SDS-PAGE) and western blot analysis

Cardiomyocytes were lysed with a cell lysis buffer (Table 6) and collected in microtubes (1.5 mL). The cell lysates were disrupted by ultrasonic processor for 3 seconds and centrifuged at 10,000 g for 10 min. Then, the protein concentration was detected by the Bradford assay (Bio-Rad). In brief, the standards or samples were added to a 96-well plate. Then, reagent A and reagent S were added to the well. In this step, proteins and copper reacted in an alkaline medium. After that, reagent B was added to the well. In this step, Folin reagent was reduced by the copper-treated protein and produced a characteristic blue color which was detected at 490 nm. The standard curve was made and the concentration of the proteins was calculated according to the color change. After that, the supernatant of cell lysates was transferred into a new tube and adjusted to the same concentration by the lysis buffer. The 6 X loading buffer (Table 7) was diluted with the supernatant of cell lysates and the protein supernatant was incubated in a metal bath at 100 °C for 5 min to denature the proteins.

Table 6: Components of Lysis Buffer (100 mL)

Tris-HCl (1M, pH=7.5)	5 mL
SDS	0.5 g
EDTA (0.5M)	200 μ L
H ₂ O	94.8 mL

Table 7: Components of 6X Loading Buffer (100 mL)

Tris-HCl (1M, pH=6.8)	37.5 mL
SDS	6 g
Bromophenol blue	30 mg
Glycerol	48 mL

β -Mercaptoethanol	9 mL
H ₂ O	5.5 mL

After preparation of protein samples, the proteins were separated by SDS-PAGE. The gel casting apparatus (Bio-Rad) was assembled and tested for leaking before the SDS-PAGE. A resolving gel (Table 8) was then prepared and the concentration of which was dependent on the size of the target protein in the samples. The mixture was transferred to the gel casting apparatus and a water overlay was filled on the top of the resolving gel to avoid the air interference. When the resolving gel had solidified after 30 min, the stacking gel was made (Table 9) and filled on the top of the resolving gel. A clean comb was inserted into the stacking gel to make space for the protein samples. The gel assembly was taken out of the casting and put into the gel tank. Running buffer (Table 10) was poured into the tank until above the top of the gel. 30 μ g protein sample was loaded in the stacking gel well. Then, the electrophoresis assembly was connected to the power supply set at 80V for 30 min and 100V for about 90 min until the running front reached the end of the gel.

Table 8: Components of Resolving Gel (10mL)

Concentration	10%	12%
H ₂ O	2.7 mL	2.05 mL
30% Acrylamide	3.35 mL	4 mL
Tris (1.5M, pH=8.8)	3.75 mL	3.75 mL
10% SDS	100 μ L	100 μ L
10% Ammonium persulfate (APS)	100 μ L	100 μ L
TEMED	4 μ L	4 μ L

Table 9: Components of Stacking Gel (3mL)

H ₂ O	2.05 mL
30% Acrylamide	0.5 mL
Tris (1.5M, pH=8.8)	0.375 mL
10% SDS	30 μ L

10% Ammonium persulfate (APS)	30 μ L
TEMED	3 μ L

Table 10: Components of Running Buffer (1L)

Tris base	3.03 g
Glycine	14.41 g
SDS	1 g
H ₂ O	1000 mL
pH	8.3

After electrophoresis, the separated proteins were transferred to a polyvinyl difluoride (PVDF) membrane (Froggabio). First, the transfer cassette equipment was immersed in transfer buffer (Table 11) and the PVDF membrane was immersed in methanol. Next, the cassettes were assembled in a sandwich structure: a sponge, a layer of blotting paper, a PVDF membrane, electrophoresed gel, a layer of blotting paper and a sponge. Then, the cassette was placed in the tank filled with transfer buffer and connected to the power supply set at 350 mA for 90 min at 4°C.

Table 11: Components of Transfer Buffer (1L)

Tris base	3.03 g
Glycine	14.41 g
Methanol	200 mL
H ₂ O	800 mL

Upon completion of the run, the PVDF membrane was removed and placed in a blocking buffer containing 5% non-fat milk at room temperature for 1 hour. The blocking buffer was made by dissolving non-fat milk (Bio Basic) in tris-buffered saline containing Tween 20 (TBST, Table 12). This step was to block the non-specific binding sites. After that, the primary antibodies were diluted with 5% bovine serum albumin (BSA, Sigma) in TBST and the PVDF membranes were incubated with the primary antibodies in a tube which was set on a rocking table at 4 °C, overnight. After incubation with the primary antibodies, the

PVDF membranes were washed 3 times with TBST for 10 min each. The membranes were then incubated with the secondary antibodies in a solution containing 5% non-fat milk in TBST at room temperature for 1 hour. After incubation with the secondary antibodies, the PVDF membranes were washed 3 times with TBST for 10 min each. Finally, the membranes were immersed in enhanced chemiluminescence (ECL) reagent (Table 13) for signal detection. The signal was visualized by an enhanced chemiluminescence-detection system.

Table 12: Components of TBST (1L)

Tris base	2.42 g
NaCl	8 g
H ₂ O	1000 mL
pH	7.6

Table 13: Components of Enhanced Chemiluminescence (ECL) Reagent (100mL)

	Reagent A	Reagent B
Tris-HCl (1M, PH=8.5)	100 mL	100 mL
Cumaric acid (90mM)	440 μ L	-
Luminol (250mM)	1 mL	-
H ₂ O ₂	-	60 μ L

Table 14: Antibody Information for Western Blot

Antibody (Polyclonal)	Company	Molecular weight (kDa)	Working
JPH2 (Mouse)	Abcam	97	1:1000
CHOP (Rabbit)	Cell Signaling	27	1:1000
GAPDH (Mouse)	Santa Cruz	37	1:400
Actin (Rabbit)	Cell Signaling	42	1:1000

2.5 Caspase-3 activity measurement

Activated caspase-3 in neonatal mouse cardiomyocytes was determined by a caspase-3 activity assay kit according to the manufacturer's protocol (BIOMOL Research

Laboratories). The cardiomyocytes were lysed with a lysis buffer (Table 15). The cell lysates were collected and centrifuged at 10,000 g for 10 min at 4 °C. The supernatant was transferred to a clean tube and the protein concentration was measured by the Bradford assay as described above. Then, 100 μ g of protein supernatant was added to the 96-well black plate. The equal volumes of assay buffer (Table 15) containing the substrate Ac-DEVD-AMC (Cayman Chemical Company) or Ac-DEVD-AMC inhibitor AC-DEVD-CHO (Cayman Chemical Company) was also added to the plate. The substrate Ac-DEVD-AMC was cleaved by caspase-3 and the released chromophore AMC was detected by a fluorescence spectrophotometer. After that, the plate was incubated at 37 °C for 2 hours and the fluorescence intensity of cleaved AMC was quantified by a fluorescence spectrophotometer with excitation of 355 nm and emission of 460 nm. The fluorescence signals were read every 30 min.

Table 15: Components of Lysis/Assay Buffer (100mL)

	Lysis buffer	Assay buffer
HEPES (1 M, pH=7.4)	5 mL	5 mL
CHAPS	0.1 g	0.1 g
NaCl	-	585 mg
DTT (1 M)	500 μ L	1 mL
EDTA (0.5 M)	20 μ L	200 μ L
NP-40	100 μ L	-
Glycerol	-	10 mL
H ₂ O	94.4 mL	83.8 mL

2.6 Cellular DNA fragmentation measurement

DNA fragmentation was detected by a Cellular DNA Fragmentation ELISA kit (Roche Applied Science) according the manufacturer's instructions. The neonatal mouse cardiomyocytes were pre-treated with BrdU labeling reagent for about 20 hours. After

various treatments, cells were washed with phosphate buffered saline (PBS, Table 16) twice and lysed with 1X incubation buffer. After incubation for 30 min at room temperature, the cell lysates were collected and centrifuged at 250 g for 10 min at 4 °C. The supernatant was collected and its protein concentration was measured by the Bradford assay. A 96-well plate was pre-coated with 1X anti-DNA antibody at 4 °C overnight. After that, the pre-coated 96-well plate was blocked with 1X incubation buffer at room temperature for 30 min. Then, the 96-well plate was washed 3 times with 1X washing buffer, 2-3 min each time. 200 μ g of protein supernatant was added into the 96-well plate for 90 min at room temperature or at 4 °C overnight. In this step, the BrdU-labeled DNA fragments bound to the immobilized anti-DNA antibody. After that, the supernatants were discarded and the 96-well plate was washed twice, 2-3 min each time. After the third wash, the 96-well plate with a washing buffer was placed in a microwave at middle power for 5 min. Then, the 96-well plate was cooled for 10 min at -20 °C. In this step, BrdU-labeled DNA fragments were denatured and fixed on the bottom of the 96-well plate. The washing buffer was discarded and the secondary antibody anti-BrdU-peroxidase was added into the 96-well plate and incubated at room temperature for 90 min. Similarly, after incubation, the reaction solution containing the secondary antibody was discarded and the 96-well plate was washed 3 times, 2-3 min each time. Then, the TMB substrate was added to each well and incubated for about 10 min at room temperature and the reaction was stopped by a stop buffer. Finally, the absorbance value in the 96-well plate was measured with excitation of 355 nm and emission of 450 nm.

Table 16: Components of PBS (1L)

NaCl	8 g
KCl	0.2 g

Na ₂ HPO ₄	3.58 g
KH ₂ PO ₄	0.24 g

2.7 Oleate/Palmitate (OA/PA) solution preparation

Stock solutions for 20 mM OA and 20 mM PA were prepared as follows. OA (Sigma) and PA (Sigma) were dissolved in 0.1 M NaOH by heating at 70°C. A 20% bovine serum albumin (BSA) solution was prepared in H₂O. The OA or PA stock solution was mixed with a 20% BSA solution followed by incubation for 10 min at 55 °C to prepare a 10 mM OA/PA-10% BSA complex solution. The complex solution was cooled to room temperature and filtered through a polyethersulfone membrane (pore size 0.1 μm) for sterilization. The complex solutions were heated for 15 min at 55 °C, then cooled to room temperature before use.

2.8 Cytoplasmic free Ca²⁺ detection

Neonatal mouse cardiomyocytes were seeded in the 96-well black plate with a transparent bottom. After various treatments, the cardiomyocytes were ready for staining. Fura-2 was a Ca²⁺ imaging dye that binds to free Ca²⁺. Fura-2 AM was the cell-permeable acetoxymethyl (AM) ester form of Fura-2. Fura-2 AM (Invitrogen) was diluted in culture medium (10% NBCS DMEM). The final concentration was 4 μM. Then, Fura-2 AM was added to the 96-well black plate and incubated at 37 °C for 60 min. The plate was washed 3 times with HBSS (Hank's balanced salt solution, Gibco) and the fluorescence intensity (R) in the 96-well black plate was measured by a fluorescence spectrophotometer with excitation of 340/380 nm and emission of 510 nm. Next, the neonatal cardiomyocytes were treated with 0.05% Triton-X 100 (Sigma) which was used to release all of the free Ca²⁺ in

cardiomyocytes to obtain the maximum fluorescence signal ($R_{\text{Triton-X 100}}$). Similarly, the fluorescence intensity was detected by a fluorescence spectrophotometer with excitation of 340/380 nm and emission of 510 nm. Then, the cardiomyocytes were treated with 20 mM EGTA (Bio Basic) to block the free Ca^{2+} which was applied to acquire the minimum fluorescence signal (R_{EGTA}). The fluorescence intensity was also determined as described before (157). Finally, the concentration of cytoplasmic free Ca^{2+} was calculated according to the formula: $[\text{Ca}^{2+}]_i = K_d \times [(R - R_{\text{EGTA}}) / (R_{\text{Triton-X 100}} - R)] \times (F_{380 \text{ EGTA}} / F_{380 \text{ Triton-X 100}})$. ($K_d = 225 \text{ nM}$, $R = F_{340} / F_{380}$)

2.9 Statistical analysis

All data were presented as mean \pm standard deviation (SD). Results were analyzed by one-way or two-way ANOVA as appropriate, followed by Fisher's LSD test or Newman-Keuls test for multi-group comparisons. A Student's t-test was used for comparison between 2 groups. The value $P < 0.05$ was considered statistically significant.

Table 17: Reagent Information

Name	Company	Cat Number
Taq DNA polymerase	FroggaBio (Toronto, Canada)	T-500
Liberase Blendzyme	Roche (Basel, Switzerland)	05401151001
DMEM	Wisent Inc (Quebec, Canada)	319010CL
NBCS	Gibco (California, America)	26010-074
Gelatin	Sigma (Missouri, America)	G9382
Ad-JPH2	Vector biolabs (Malvern, America)	ADV-212592
Ad-shJPH2	Vector biolabs (Malvern, America)	Customized
Ad-GFP	SignaGen laboratories (Rockville, America)	SL100708
Ad-HA	Vector biolabs (Malvern, America)	ADV-294343
Bradford assay	Bio-Rad (California, America)	500-0001

PVDF membrane	Froggabio (Toronto, Canada)	TM300
Non-fat milk	Bio Basic (Toronto, Canada)	NB0669
Tween 20	Sigma (Missouri, America)	P9416
BSA	Sigma (Missouri, America)	A9647
Ac-DEVD-AMC	Cayman Chemical (Michigan, America)	14986
Ac-DEVD-CHO	Cayman Chemical (Michigan, America)	10017
DNA fragmentation	Roche (Basel, Switzerland)	11585045001
Oleate	Sigma (Missouri, America)	O7501
Palmitate	Sigma (Missouri, America)	P9767
Fura-2 AM	eBioscience (California, America)	65085839
HBSS	Gibco (California, America)	14065056
Triton X-100	Sigma (Missouri, America)	T9284
EGTA	Bio Basic (Toronto, Canada)	ED0077
NaOH	VWR (Pennsylvania, America)	BDH7222-1
EDTA	Sigma (Missouri, America)	E5134
Tris	Bio Basic (Toronto, Canada)	TB0196
HCl	Sigma (Missouri, America)	HX0603-4
KCl	Sigma (Missouri, America)	PX1405-1
KH ₂ PO ₄	Bio Basic (Toronto, Canada)	PB0445
NaCl	Bio Basic (Toronto, Canada)	DB0483
D-Glucose	Bio Basic (Toronto, Canada)	GB0219
Phenol red	Sigma (Missouri, America)	P5530
SDS	Sigma (Missouri, America)	L3771
Bromophenol Blue	Sigma (Missouri, America)	20017
Glycerol	Sigma (Missouri, America)	G5516
β-Mercaptoethanol	Sigma (Missouri, America)	444203
Acrylamide	Bio Basic (Toronto, Canada)	AB1032
APS	Bio Basic (Toronto, Canada)	AB0072
TEMED	Bio Basic (Toronto, Canada)	TB 0508
Glycine	Bio Basic (Toronto, Canada)	GB0235
Methanol	VWR (Pennsylvania, America)	BDH1135-4LP
Coumeric acid	Sigma (Missouri, America)	C9008
Luminol	Sigma (Missouri, America)	A8511
HEPES	Bio Basic (Toronto, Canada)	HB0264
CHAPS	Bio Basic (Toronto, Canada)	CD0110

DTT	Bio Basic (Toronto, Canada)	DB0058
NP-40	Sigma (Missouri, America)	13021
Na ₂ HPO ₄	Sigma (Missouri, America)	S0876
Ryanodine	Abcam (Cambridge, England)	ab120083

Chapter 3

3 Results

3.1 Palmitate incubation increases caspase-3 activity in cultured neonatal mouse cardiomyocytes

It was reported that palmitate was able to cause apoptosis in cardiomyocytes (*158-161*). To confirm this finding in our study, neonatal mouse cardiomyocytes were treated with palmitate (PA), a main saturated free fatty acid in western diet, and oleate (OA) served as a control. Palmitate has been widely applied in the study of cardiac lipotoxicity. Most of the studies show that the concentration of palmitate ranges from 100 μM to 1200 μM (*162-168*). We tried 200 μM , 400 μM and 800 μM palmitate to treat neonatal cardiomyocytes and found the concentration of 800 μM showed the best induction of apoptosis in cardiomyocytes compared to oleate. Since then, we used this concentration of palmitate for the following studies. Neonatal mouse cardiomyocytes were treated with PA (800 μM) or OA (800 μM) for 48 hours. Then, caspase-3 activity was measured to indicate the apoptosis in cardiomyocytes. Palmitate incubation increased caspase-3 activity by 60% in neonatal cardiomyocytes compared to OA group (Figure 3).

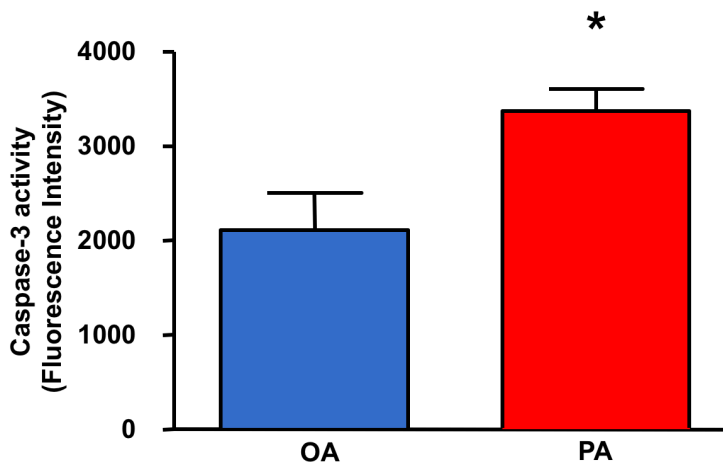


Figure 3: Palmitate incubation increases caspase-3 activity in neonatal mouse cardiomyocytes.

Neonatal mouse cardiomyocytes were isolated and cultured for 24 hours. After incubation with oleate (OA) or palmitate (PA) for 48 hours, the apoptosis in neonatal mouse cardiomyocytes was analyzed by the measurement of caspase-3 activity. Data was mean \pm SD from 4 independent experiments and analyzed by unpaired Student's t-test. * $P < 0.05$ versus OA.

3.2 Palmitate incubation increases DNA fragmentation in cultured neonatal mouse cardiomyocytes

Neonatal mouse cardiomyocytes were treated with PA (800 μ M) or OA (800 μ M) for 48 hours. Then, DNA fragmentation was measured to indicate the apoptosis in cardiomyocytes. PA incubation increased DNA fragmentation by 50% in neonatal cardiomyocytes relative to OA group (Figure 4). These results (Figure 3 and 4) confirmed that palmitate incubation induces apoptosis in cultured neonatal mouse cardiomyocytes when compared to oleate.

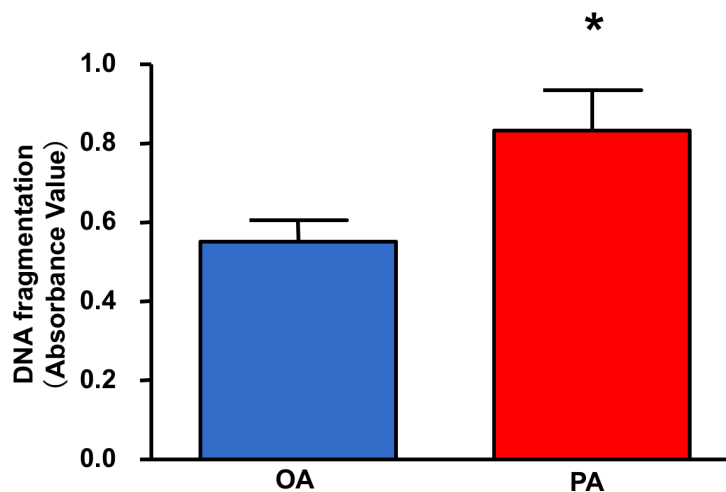


Figure 4: Palmitate incubation increases DNA fragmentation in neonatal mouse cardiomyocytes.

Neonatal mouse cardiomyocytes were isolated and cultured for 24 hours. After incubation with oleate (OA) or palmitate (PA) for 48 hours, the apoptosis in neonatal mouse cardiomyocytes was analyzed by the measurement of DNA fragmentation. Data was mean \pm SD from 3 independent experiments and analyzed by unpaired Student's t-test. * $P < 0.05$ versus OA.

3.3 Palmitate incubation reduces JPH2 expression in cultured neonatal mouse cardiomyocytes

The expression of JPH2 was down-regulated in many cardiac diseases (35, 36). Prior study from our lab showed that the protein levels of JPH2 were reduced in the hearts of mice fed with high fat diet for 4 months (2). To confirm this, neonatal mouse cardiomyocytes were treated with 800 uM PA or OA for 48 hours. The protein levels of JPH2 were determined by western blot analysis. PA incubation decreased JPH2 expression by 30% in neonatal mouse cardiomyocytes compared to OA group (Figure 5). This result indicated that palmitate incubation reduces JPH2 expression in neonatal mouse cardiomyocytes when compared to oleate.

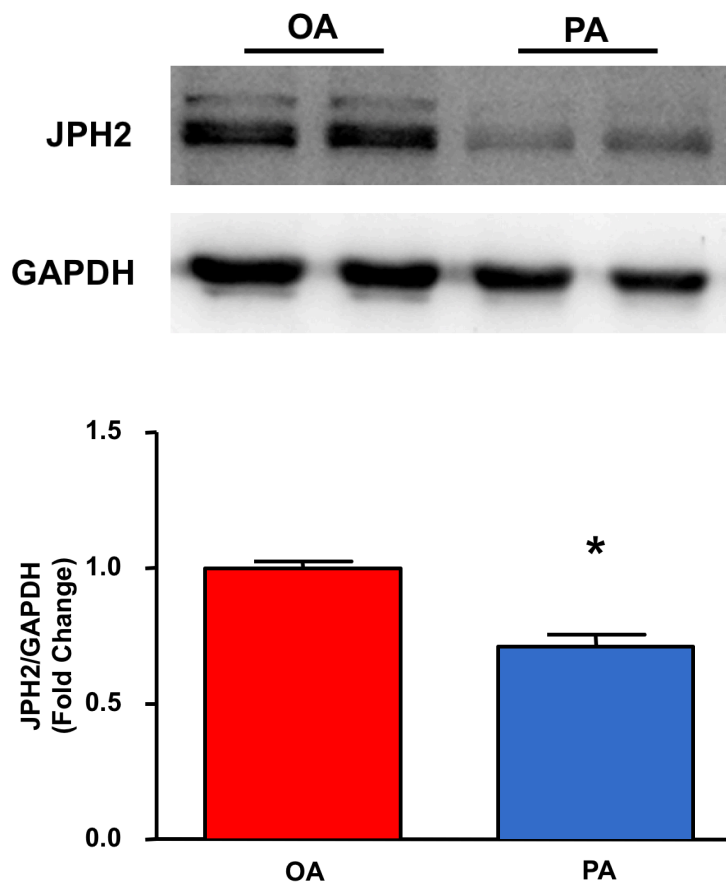


Figure 5: Palmitate incubation reduces JPH2 protein expression in neonatal mouse cardiomyocytes.

Neonatal mouse cardiomyocytes were isolated and cultured for 24 hours. After incubation with oleate (OA) or palmitate (PA) for 48 hours, the protein levels of JPH2 were analyzed by western blot analysis. GAPDH was used as a loading control. Upper panel: a representative western blot for JPH2 and GAPDH from 4 different cultures with each in duplicate; lower panel: quantitation of the protein levels of JPH2 relative to GAPDH. Data was mean \pm SD from 4 independent experiments and analyzed by unpaired Student's t-test. * $P < 0.05$ versus OA.

3.4 Knockdown of JPH2 in cultured neonatal mouse cardiomyocytes

To study the influence of JPH2 down-regulation in neonatal mouse cardiomyocytes, we used an adenoviral vector containing shJPH2 (Ad-shJPH2) to knock down JPH2. An adenoviral vector containing GFP (Ad-GFP) served as a control. Neonatal mouse cardiomyocytes were infected with Ad-shJPH2 (30, 60 or 100 PFU/cell) or Ad-GFP (100 PFU/cell). 48 hours later, the protein levels of JPH2 were determined by western blot analysis. The protein levels of JPH2 were reduced in cardiomyocytes infected with Ad-shJPH2 compared to Ad-GFP group by 30%, 60% and 80% (Figure 6). This result indicated a successful knockdown of JPH2 by Ad-shJPH2 in cardiomyocytes. Since the dose of 100 PFU/cell showed the best knockdown of JPH2, we used this dose of Ad-shJPH2 for the following studies.

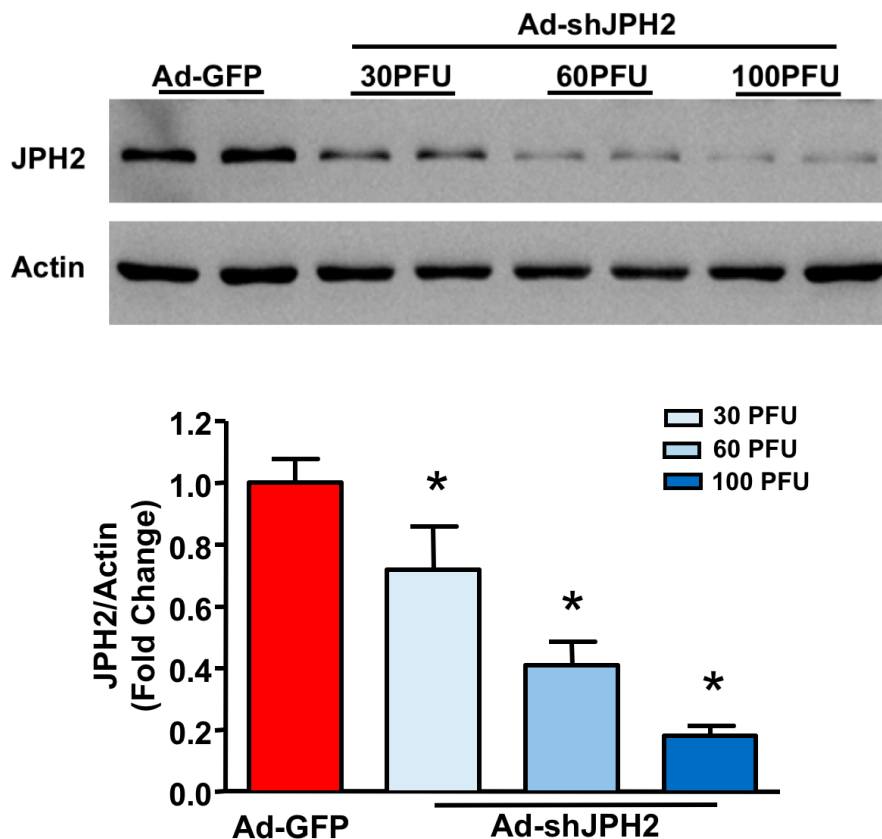


Figure 6: Knockdown of JPH2 with Ad-shJPH2 in neonatal mouse cardiomyocytes.

Neonatal mouse cardiomyocytes were isolated and cultured for 24 hours. The cells were infected with Ad-shJPH2 or Ad-GFP. 48 hours later, the protein levels of JPH2 in neonatal cardiomyocytes were analyzed by western blot. Actin was used as a loading control. Upper panel: a representative western blot for JPH2 and Actin from 3 different cultures with each in duplicate. Lower panel: quantitation of the protein levels of JPH2 relative to Actin. Data was mean \pm SD from 3 independent experiments, and analyzed by one-way ANOVA followed by Fisher's LSD test.

* $P < 0.05$ versus Ad-GFP.

3.5 JPH2 knockdown enhances palmitate-induced caspase-3 activity in cultured neonatal mouse cardiomyocytes

To investigate whether JPH2 knockdown enhanced palmitate-induced cardiomyocyte injury, we knocked down JPH2 in cardiomyocytes and treated the cardiomyocytes with PA. Neonatal mouse cardiomyocytes were infected with Ad-shJPH2 (100 PFU/cell) or Ad-GFP (100 PFU/cell) for 24 hours and then treated with 800 μ M PA or OA for another 24 hours. The caspase-3 activity was measured to indicate apoptosis. Knockdown of JPH2 solely induced higher caspase-3 activity by 330% compared to the Ad-GFP group, indicating apoptotic cell death. Similarly, treatment with PA solely also resulted in higher caspase-3 activity by 100% compared with OA group. Furthermore, palmitate-induced apoptosis was enhanced by knockdown of JPH2 by 160% as determined by caspase-3 activity (Figure 7).

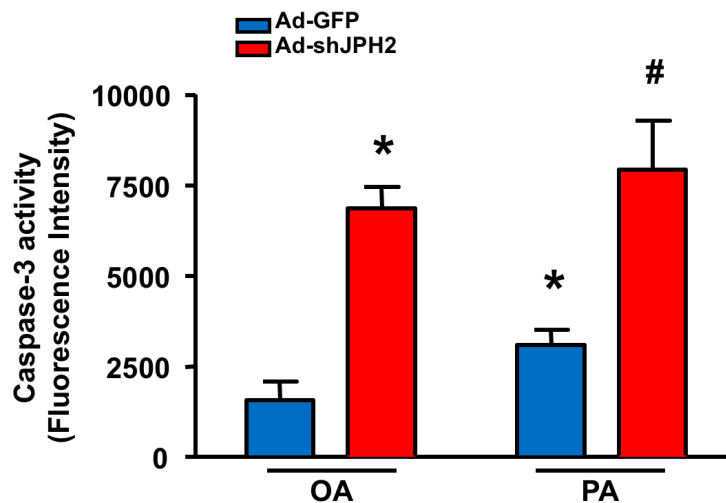


Figure 7: JPH2 knockdown enhances palmitate-induced caspase-3 activity in neonatal mouse cardiomyocytes.

Neonatal mouse cardiomyocytes were isolated and cultured for 24 hours. After infection with Ad-shJPH2 or Ad-GFP, together with incubation with oleate (OA) or palmitate (PA) for 48 hours, apoptosis in neonatal mouse cardiomyocytes was analyzed by the measurement of caspase-3 activity. Data was mean \pm SD from 5 independent experiments and analyzed by two-way ANOVA followed by Newman-Keuls test. * $P < 0.05$ versus OA-Ad-GFP, # $P < 0.05$ versus PA-Ad-GFP.

3.6 JPH2 knockdown enhances palmitate-induced DNA fragmentation in cultured neonatal mouse cardiomyocytes

Neonatal mouse cardiomyocytes were infected with Ad-shJPH2 (100 PFU/cell) or Ad-GFP (100 PFU/cell) for 24 hours and then treated with 800 μ M PA or OA for another 24 hours. DNA fragmentation was measured to indicate the apoptosis. Knockdown of JPH2 solely induced greater DNA fragmentation by 100% compared to Ad-GFP group, indicating apoptotic cell death. Similarly, treatment of PA solely also induced greater DNA fragmentation by 40% compared to OA group. Furthermore, palmitate-induced apoptosis was exacerbated by JPH2 knockdown by 65% as measured by DNA fragmentation (Figure 8). These results (Figure 7 and 8) demonstrated that JPH2 knockdown enhances palmitate-induced apoptosis in neonatal cardiomyocytes.

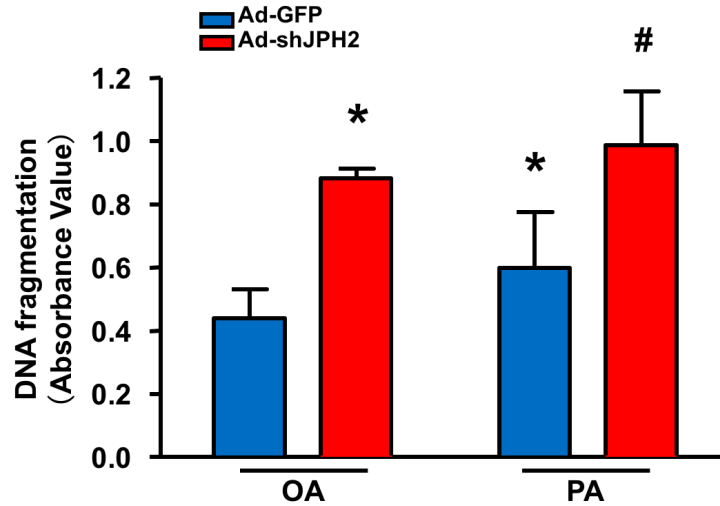


Figure 8: JPH2 knockdown enhances palmitate-induced DNA fragmentation in neonatal mouse cardiomyocytes.

Neonatal mouse cardiomyocytes were isolated and cultured for 24 hours. After infection with Ad-shJPH2 or Ad-GFP, together with incubation with oleate (OA) or palmitate (PA) for 48 hours, apoptosis in neonatal mouse cardiomyocytes was analyzed by the measurement of DNA fragmentation. Data was mean \pm SD from 3 independent experiments and analyzed by two-way ANOVA followed by Newman Keuls test. * $P < 0.05$ versus OA-Ad-GFP, # $P < 0.05$ versus PA-Ad-GFP.

3.7 Over-expression of JPH2 in cultured neonatal mouse cardiomyocytes

To up-regulate JPH2 expression, we used an adenoviral vector containing JPH2 (Ad-JPH2). An adenoviral vector containing human influenza hemagglutinin (aa 98-106) peptide tag (Ad-HA) served as a control. Neonatal mouse cardiomyocytes were infected with Ad-JPH2 (10, 20 and 40 PFU/cell) or Ad-HA (40 PFU/cell). 48 hours later, the protein levels of JPH2 were determined by western blot analysis. The protein levels of JPH2 were higher by 40%, 200% and 300% in cardiomyocytes infected with Ad-JPH2 compared to Ad-HA group (Figure 9). This result indicated a successful over-expression of JPH2 by Ad-JPH2 in cardiomyocytes. Since the dose of 40 PFU/cell showed the best over-expression of JPH2, we used this dose of Ad-JPH2 for the following studies.

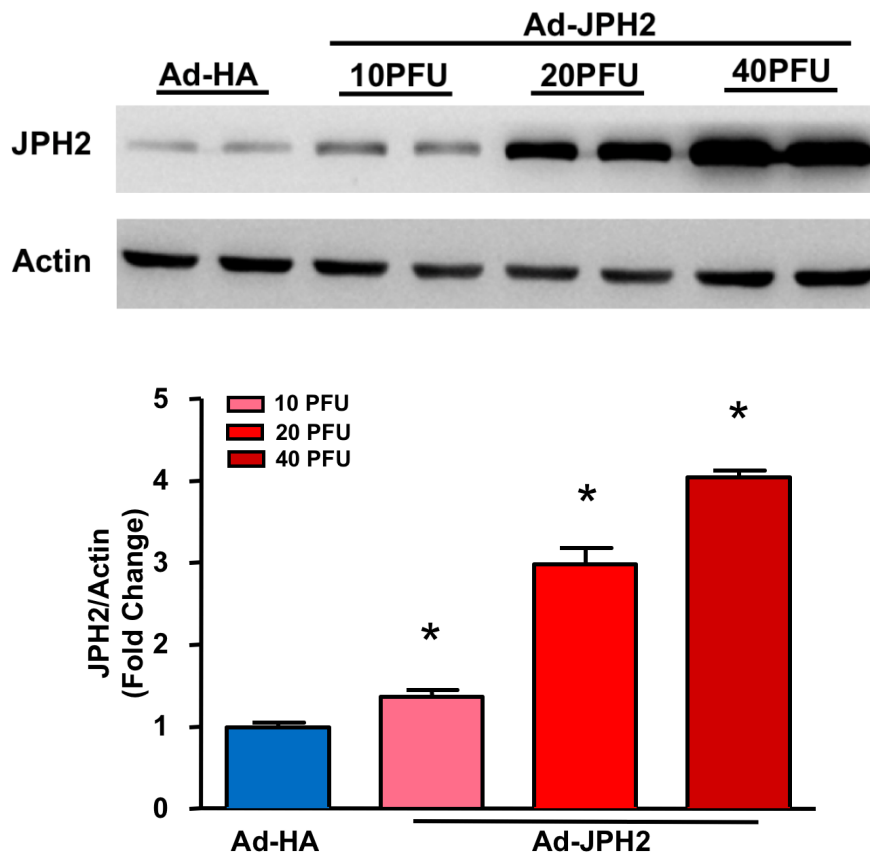


Figure 9: Over-expression of JPH2 with Ad-JPH2 in neonatal mouse cardiomyocytes.

Neonatal mouse cardiomyocytes were isolated and cultured for 24 hours. After infection with Ad-JPH2 or Ad-HA for 48 hours, the protein levels of JPH2 in neonatal cardiomyocytes were analyzed by western blot. Actin was used as a loading control. Upper panel: a representative western blot for JPH2 and Actin from 3 different cultures, each in duplicate. Lower panel: quantitation of the protein levels of JPH2 relative to Actin. Data was mean \pm SD from 3 independent experiments and analyzed by one-way ANOVA followed by Fisher's LSD test.

* $P < 0.05$ versus Ad-HA.

3.8 JPH2 over-expression attenuates palmitate-induced caspase-3 activity in cultured neonatal mouse cardiomyocytes

To determine whether JPH2 over-expression had a protective role in palmitate-induced cell injury, we over-expressed JPH2 in cardiomyocytes and treated the cardiomyocytes with PA. Neonatal mouse cardiomyocytes were infected with Ad-JPH2 (40 PFU/cell) or Ad-HA (40 PFU/cell) for 24 hours and then treated with 800 μ M PA or OA for another 24 hours. Caspase-3 activity was measured to indicate the apoptosis. JPH2 over-expression solely reduced caspase-3 activity by 60% compared to Ad-HA group. PA treatment resulted in greater caspase-3 activity by 50% in neonatal cardiomyocytes compared to OA group, indicative of apoptotic cell death. However, PA-induced caspase-3 activity was attenuated by the over-expression of JPH2 by 60% in neonatal cardiomyocytes (Figure 10).

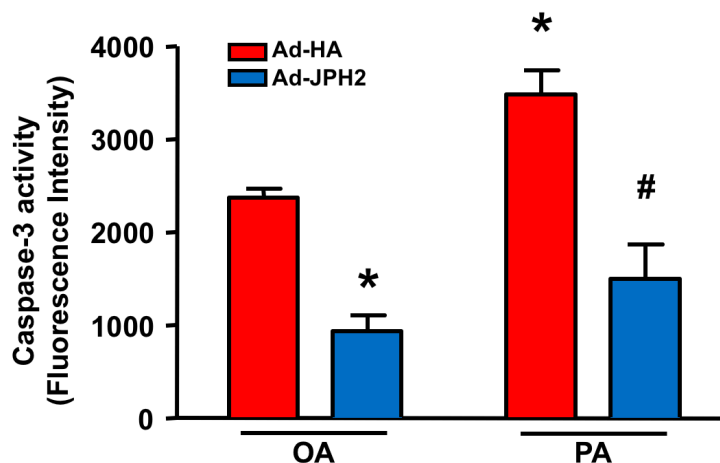


Figure 10: JPH2 over-expression attenuates palmitate-induced caspase-3 activity in neonatal mouse cardiomyocytes.

Neonatal mouse cardiomyocytes were isolated and cultured for 24 hours. After infection with Ad-JPH2 or Ad-HA, together with incubation with oleate (OA) or palmitate (PA) for 48 hours, apoptosis in neonatal mouse cardiomyocytes was analyzed by the measurement of caspase-3 activity. Data was mean \pm SD from 4 independent experiments and analyzed by two-way ANOVA followed by Newman-Keuls test. * $P < 0.05$ versus OA-Ad-HA, # $P < 0.05$ versus PA-Ad-HA.

3.9 JPH2 over-expression attenuates palmitate-induced DNA fragmentation in cultured neonatal mouse cardiomyocytes

Neonatal mouse cardiomyocytes were infected with Ad-JPH2 (40 PFU/cell) or Ad-HA (40 PFU/cell) for 24 hours and then treated with 800 μ M PA or OA for another 24 hours. DNA fragmentation was further measured to indicate the apoptosis. JPH2 over-expression solely reduced DNA fragmentation by 50% compared to Ad-HA group. PA treatment resulted in greater DNA fragmentation by 50% in neonatal cardiomyocytes relative to OA group, indicating of apoptotic cell death. In contrast, PA-induced DNA fragmentation was attenuated by the over-expression of JPH2 by 50% in neonatal cardiomyocytes (Figure 11). These results (Figure 10 and 11) indicated that JPH2 over-expression attenuates palmitate-induced apoptosis in neonatal cardiomyocytes.

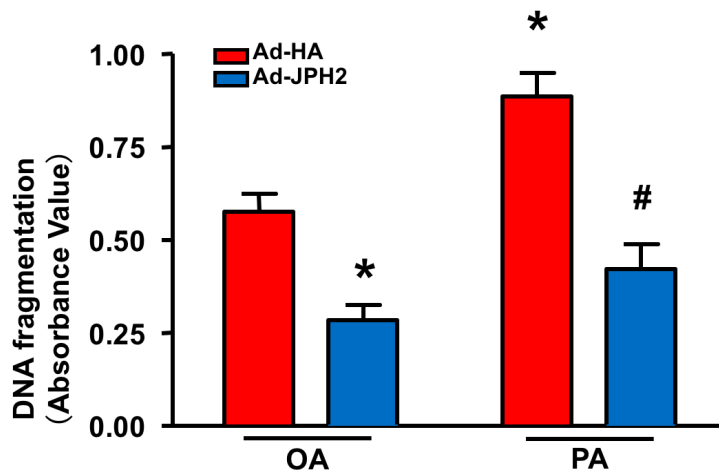


Figure 11: JPH2 over-expression attenuates palmitate-induced DNA fragmentation in neonatal mouse cardiomyocytes.

Neonatal mouse cardiomyocytes were isolated and cultured for 24 hours. After infection with Ad-JPH2 or Ad-HA, together with incubation with oleate (OA) or palmitate (PA) for 48 hours, apoptosis in neonatal mouse cardiomyocytes was analyzed by the measurement of DNA fragmentation. Data was mean \pm SD from 3 independent experiments and analyzed by two-way ANOVA followed by Newman Keuls test. * $P < 0.05$ versus OA-Ad-HA, # $P < 0.05$ versus PA-Ad-HA.

3.10 Knockdown of JPH2 induces caspase-3 activity in cultured neonatal mouse cardiomyocytes

We had successfully knocked down JPH2 by Ad-shJPH2 in neonatal mouse cardiomyocytes. Next, we wanted to determine whether JPH2 knockdown sufficiently induced apoptosis in cardiomyocytes. Similarly, we used Ad-shJPH2 to knockdown JPH2 and Ad-GFP served as a control. Neonatal cardiomyocytes were infected with Ad-shJPH2 (100 PFU/cell) or Ad-GFP (100 PFU/cell) for 48 hours. Apoptosis was assessed by measuring caspase-3 activity which was the most frequently activated death protease in the execution phase of apoptosis. JPH2 knockdown resulted in greater caspase-3 activity by 210% in neonatal cardiomyocytes infected with Ad-shJPH2 compared to Ad-GFP group (Figure 12).

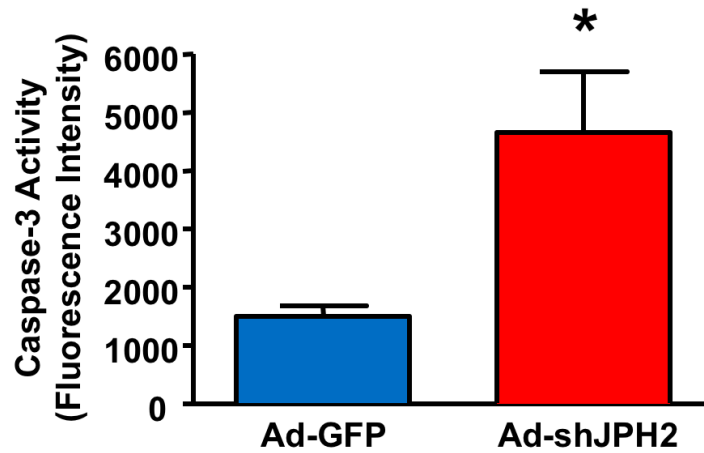


Figure 12: JPH2 knockdown induces caspase-3 activity in neonatal mouse cardiomyocytes.

Neonatal mouse cardiomyocytes were isolated and cultured for 24 hours. After infection with Ad-shJPH2 or Ad-GFP for 48 hours, apoptosis in neonatal mouse cardiomyocytes was determined by the detection of caspase-3 activity. Data was mean \pm SD from 4 independent experiments and analyzed by unpaired Student's t-test. * $P < 0.05$ versus Ad-GFP.

3.11 Knockdown of JPH2 increases DNA fragmentation in cultured neonatal mouse cardiomyocytes

Neonatal cardiomyocytes were infected with Ad-shJPH2 (100 PFU/cell) or Ad-GFP (100 PFU/cell) for 48 hours. Apoptosis was further analyzed by measuring DNA fragmentation, which was also a biological hallmark of apoptosis. JPH2 knockdown resulted in greater DNA fragmentation by 90% in neonatal cardiomyocytes infected with Ad-shJPH2 compared to Ad-GFP group (Figure 13). These results (Figure 12 and 13) demonstrated that knockdown of JPH2 sufficiently induces apoptosis in cultured neonatal mouse cardiomyocytes relative to Ad-GFP group.

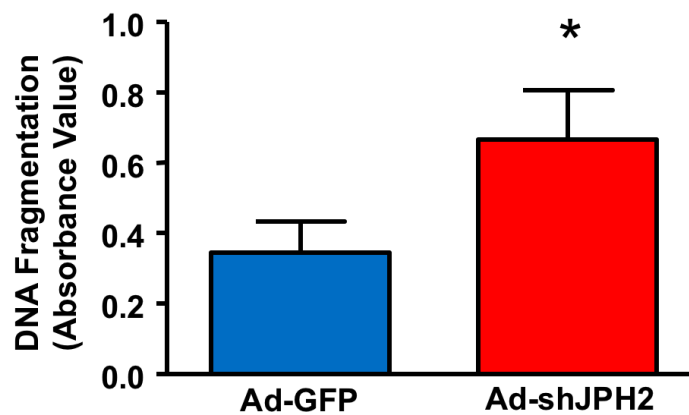


Figure 13: JPH2 knockdown induces DNA fragmentation in neonatal mouse cardiomyocytes.

Neonatal mouse cardiomyocytes were isolated and cultured for 24 hours. After infection with Ad-shJPH2 or Ad-GFP for 48 hours, apoptosis in neonatal mouse cardiomyocytes was determined by the detection of DNA fragmentation. Data was mean \pm SD from 3 independent experiments and analyzed by unpaired Student's t-test. * $P < 0.05$ versus Ad-GFP.

3.12 Palmitate incubation increases CHOP expression in cultured neonatal mouse cardiomyocytes

To investigate whether palmitate incubation induced ER stress in cardiomyocytes, neonatal mouse cardiomyocytes were subjected to palmitate incubation. Neonatal mouse cardiomyocytes were treated with 800 μ M PA or OA for 24 hours. The protein levels of CHOP were determined by western blot as an indicator of ER stress. Similarly, PA treatment also induced higher CHOP expression by 120% in neonatal cardiomyocytes compared to OA group (Figure 14). This result demonstrated that palmitate incubation results in higher CHOP expression, indicating palmitate incubation induces ER stress in neonatal cardiomyocytes compared to oleate.

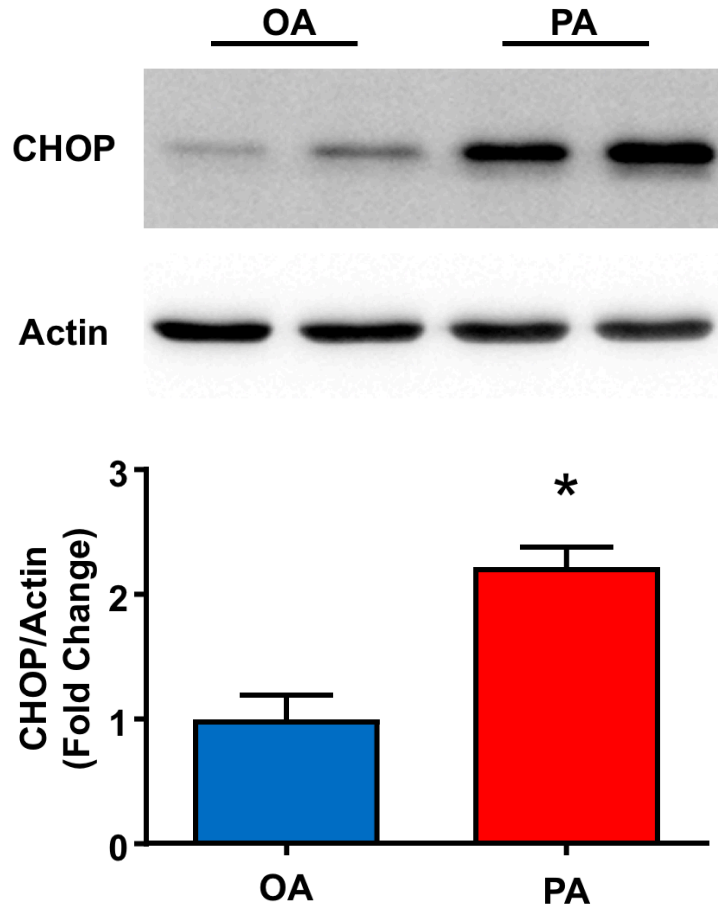


Figure 14: Palmitate incubation increases CHOP protein expression in neonatal mouse cardiomyocytes.

Neonatal mouse cardiomyocytes were isolated and cultured for 24 hours. After incubation with oleate (OA) or palmitate (PA) for 24 hours, the protein levels of CHOP were analyzed by western blot. Actin was used as a loading control. Upper panel: a representative western blot for CHOP and actin from 4 different cultures in duplicate. Lower panel: quantitation of the protein levels of CHOP relative to actin. Data was mean \pm SD from 4 independent experiments and analyzed by unpaired Student's t-test. * $P < 0.05$ versus OA.

3.13 JPH2 knockdown increases CHOP expression in cultured neonatal mouse cardiomyocytes

To determine whether JPH2 knockdown induced ER stress in cardiomyocytes, neonatal mouse cardiomyocytes were subjected to Ad-shJPH2 infection. Neonatal mouse cardiomyocytes were infected with Ad-shJPH2 (100 PFU/cell) or Ad-GFP (100 PFU/cell) for 24 hours. CHOP was detected to indicate the ER stress in neonatal cardiomyocytes. The protein levels of CHOP were determined by western blot. JPH2 knockdown resulted in higher CHOP expression by 60% in neonatal cardiomyocytes compared to Ad-GFP group (Figure 15).

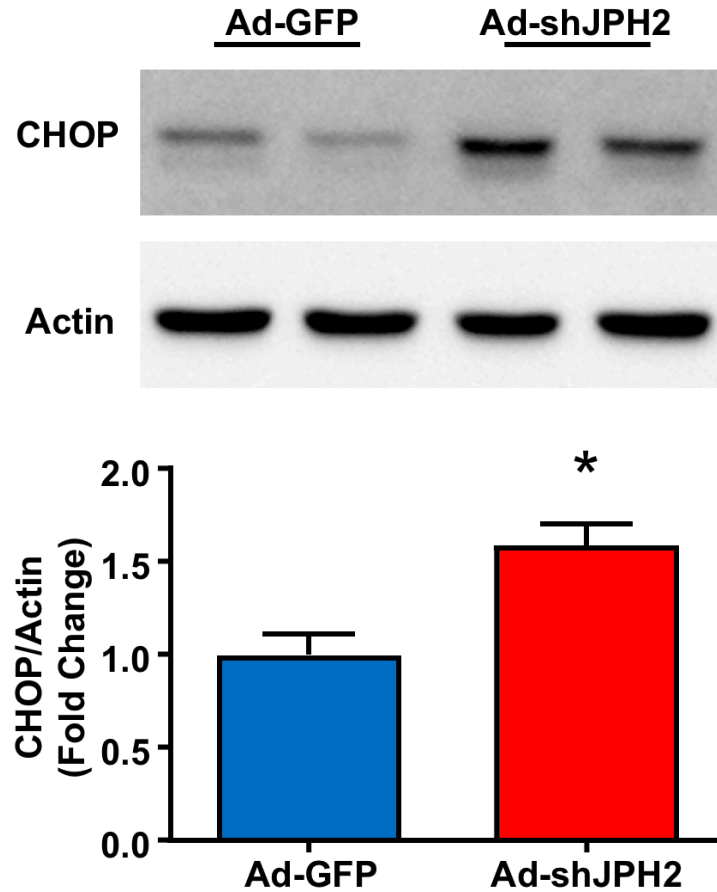


Figure 15: JPH2 knockdown increases CHOP protein expression in neonatal mouse cardiomyocytes.

Neonatal mouse cardiomyocytes were isolated and cultured for 24 hours. After infection with Ad-GFP/Ad-shJPH2 for 24 hours, the protein levels of CHOP were analyzed by western blot. Actin was used as a loading control. Upper panel: a representative western blot for CHOP and actin from 4 different cultures with each in duplicate. Lower panel: quantitation of the protein levels of CHOP relative to actin. Data was mean \pm SD from 4 independent experiments and analyzed by unpaired Student's t-test. * $P < 0.05$ versus Ad-GFP.

3.14 Over-expression of JPH2 attenuates palmitate-induced CHOP expression in cultured neonatal mouse cardiomyocytes

We had shown that both JPH2 knockdown and palmitate incubation induced ER stress and apoptosis in cardiomyocytes, and over-expression of JPH2 protected cardiomyocytes against palmitate-induced apoptosis. Therefore, we were curious whether this protective role of JPH2 was dependent on preventing ER stress. To investigate if JPH2 over-expression attenuated palmitate-induced ER stress in cardiomyocytes, we over-expressed JPH2 in neonatal cardiomyocytes first and then treated the cardiomyocytes with palmitate. Neonatal mouse cardiomyocytes were infected with Ad-JPH2 (40 PFU/cell) or Ad-HA (40 PFU/cell) for 24 hours. Then, the cardiomyocytes were treated with 800 μ M PA or OA for 24 hours. CHOP expression was detected to indicate the ER stress in neonatal cardiomyocytes. The protein levels of CHOP were determined by western blot. PA treatment resulted in greater CHOP expression by 260% in cardiomyocytes compared to OA group, indicating of ER stress. JPH2 over-expression prevented palmitate-induced CHOP expression by 40% in neonatal cardiomyocytes (Figure 16). This result indicated that JPH2 over-expression attenuates palmitate-induced ER stress in neonatal cardiomyocytes.

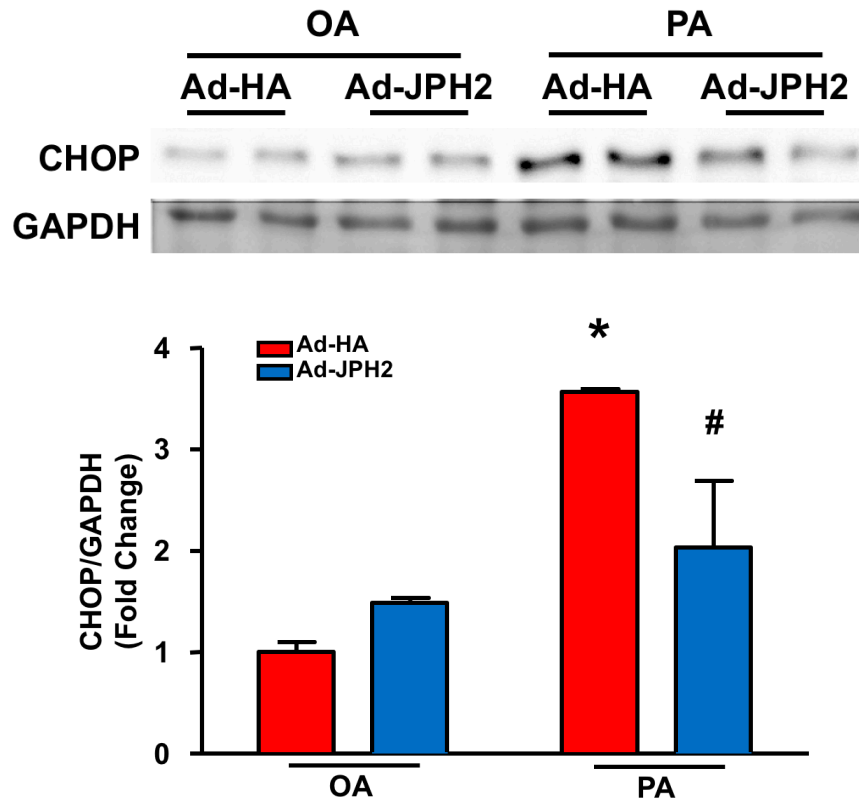


Figure 16: JPH2 over-expression attenuates palmitate-induced CHOP protein expression in neonatal mouse cardiomyocytes.

Neonatal mouse cardiomyocytes were isolated and cultured for 24 hours. After infection with Ad-JPH2 or Ad-HA and incubation with oleate (OA) or palmitate (PA), the protein levels of CHOP were analyzed by western blot. GAPDH was used as a loading control. Upper panel: a representative western blot for CHOP and GAPDH from 3 different cultures in duplicate. Lower panel: quantitation of the protein levels of CHOP relative to GAPDH. Data was mean \pm SD from 3 independent experiments and analyzed by two-way ANOVA followed by Newman-Keuls test. * $P < 0.05$ versus OA-Ad-HA, # $P < 0.05$ versus PA-Ad-HA.

3.15 CHOP knockout reduces JPH2 knockdown-induced caspase-3 activity in cultured neonatal mouse cardiomyocytes

To determine if JPH2 knockdown induced apoptosis by CHOP up-regulation in cardiomyocytes, we isolated neonatal cardiomyocytes from wild type (WT) or CHOP knockout (CHOP^{-/-}) mice. Neonatal mouse cardiomyocytes from WT/CHOP^{-/-} mice were infected with Ad-shJPH2 (100 PFU/cell) or Ad-GFP (100 PFU/cell) for 48 hours. Then, caspase-3 activity was measured to indicate apoptosis in cardiomyocytes. As observed earlier, JPH2 knockdown resulted in greater caspase-3 activity by 210% in WT cardiomyocytes (Figure 17). CHOP knockout resulted in lower JPH2 knockdown-induced caspase-3 activity by 15% in neonatal cardiomyocytes (Figure 17).

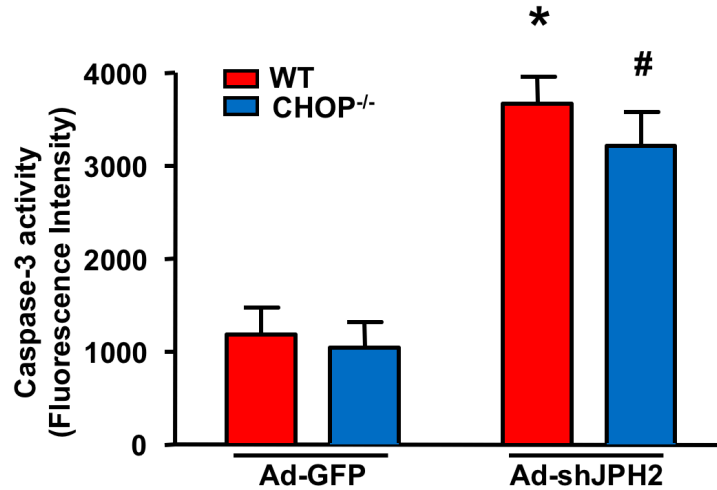


Figure 17: CHOP knockout reduces JPH2 knockdown-induced caspase-3 activity in neonatal mouse cardiomyocytes.

Neonatal mouse cardiomyocytes were isolated and cultured for 24 hours. After infection with Ad-shJPH2 or Ad-GFP for 48 hours, caspase-3 activity was analyzed in neonatal mouse cardiomyocytes from WT/CHOP^{-/-} mice. Data was mean \pm SD from 8 independent experiments and analyzed by two-way ANOVA followed by Newman Keuls test. * $P < 0.05$ versus Ad-GFP-WT, # $P < 0.05$ versus Ad-shJPH2-WT.

3.16 CHOP knockout reduces palmitate-induced caspase-3 activity in cultured neonatal mouse cardiomyocytes

To determine if palmitate induced apoptosis through CHOP up-regulation in cardiomyocytes, we isolated neonatal cardiomyocytes from wild type (WT) or CHOP knockout (CHOP^{-/-}) mice. Neonatal cardiomyocytes from WT/CHOP^{-/-} mice were treated with 800 μ M PA or OA for 48 hours. Then, caspase-3 activity was measured to indicate apoptosis in cardiomyocytes. CHOP knockout solely reduced caspase-3 activity by 40% compared to WT cardiomyocytes. PA incubation resulted in greater caspase-3 activity by 70% in WT cardiomyocytes when compared to oleate (Figure 18). CHOP knockout attenuated palmitate-induced caspase-3 activity by 40% in neonatal cardiomyocytes (Figure 18). These results (Figure 17 and 18) indicated that CHOP knockout reduces JPH2 knockdown or palmitate-induced caspase-3 activity, indicating CHOP induction is an important factor contributing to apoptosis caused by JPH2 knockdown or palmitate incubation.

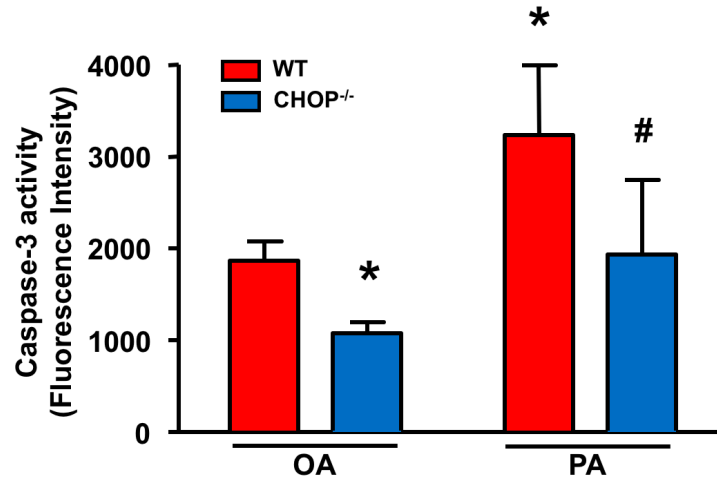


Figure 18: CHOP knockout reduces palmitate-induced caspase-3 activity in neonatal mouse cardiomyocytes.

Neonatal mouse cardiomyocytes were isolated and cultured for 24 hours. After incubation with oleate (OA) or palmitate (PA) for 48 hours, caspase-3 activity was determined in neonatal cardiomyocytes from WT/CHOP^{-/-} mice. Data was mean \pm SD from 8 independent experiments and analyzed by two-way ANOVA followed by Newman Keuls test. * $P < 0.05$ versus OA-WT, # $P < 0.05$ versus PA-WT.

3.17 Inhibition of Ca^{2+} release from RyR2 reduces palmitate-induced CHOP expression in cultured neonatal mouse cardiomyocytes

To determine whether palmitate induced CHOP expression through Ca^{2+} release from RyR2, we used ryanodine to block Ca^{2+} release from RyR2 in cardiomyocytes. To do this, neonatal cardiomyocytes were treated with 800 μM PA or OA for 24 hours together with incubation with ryanodine (0, 10 and 50 μM). The protein levels of CHOP were determined by western blot to indicate ER stress. Palmitate incubation resulted in greater expression of CHOP by 100% in cardiomyocytes when compared to oleate (Figure 19). Ryanodine resulted in lower palmitate-induced CHOP expression by 30% and 50% in neonatal cardiomyocytes (Figure 19). These results demonstrated that inhibition of Ca^{2+} release from RyR2 prevents palmitate incubation-induced CHOP expression, indicating disruption of Ca^{2+} homeostasis participates in palmitate incubation-induced ER stress in cardiomyocytes.

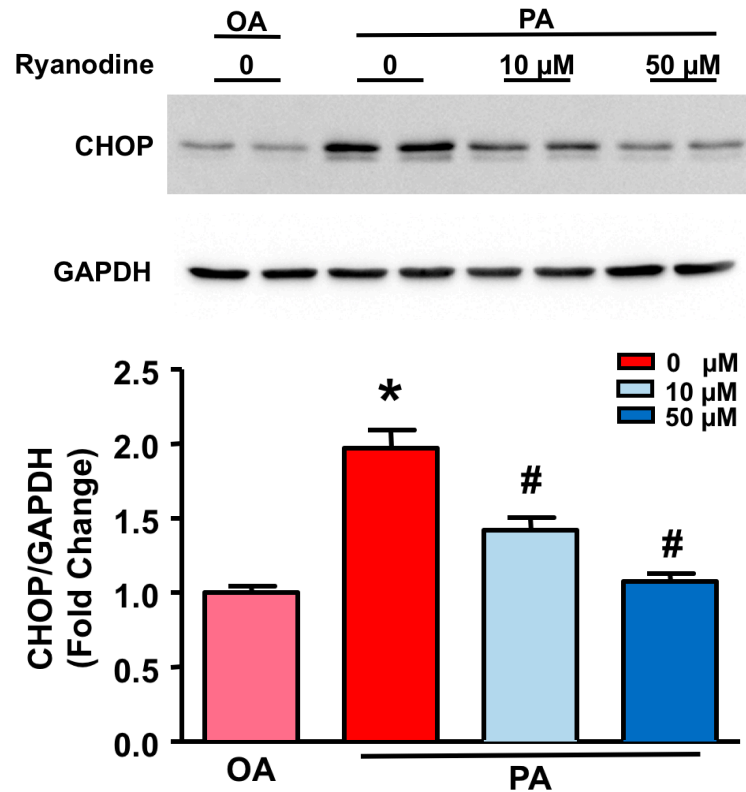


Figure 19: Inhibition of Ca^{2+} release from RyR2 reduces palmitate-induced CHOP protein expression in neonatal mouse cardiomyocytes.

Neonatal mouse cardiomyocytes were isolated and cultured for 24 hours. After incubation with oleate (OA) or palmitate (PA) with or without ryanodine treatment for 24 hours, the protein levels of CHOP were analyzed by western blot analysis. GAPDH was used as a loading control. Upper panel: a representative western blot for CHOP and GAPDH from 4 different cultures in duplicate. Lower panel: quantitation of the protein levels of CHOP relative to GAPDH. Data was mean \pm SD from 4 independent experiments and analyzed by two-way ANOVA followed by Newman-Keuls test. * $P < 0.05$ versus OA-0 μM ryanodine, # $P < 0.05$ versus PA-0 μM ryanodine.

3.18 Inhibition of Ca^{2+} release from RyR2 reduces JPH2 knockdown-induced CHOP expression in cultured neonatal mouse cardiomyocytes

To determine if JPH2 knockdown induced CHOP expression through Ca^{2+} release from RyR2 in cardiomyocytes, neonatal mouse cardiomyocytes were infected with Ad-shJPH2 (100 PFU/cell) or Ad-GFP (100 PFU/cell) for 24 hours. At the same time, neonatal cardiomyocytes were treated with ryanodine (0, 10 and 50 μM). The protein levels of CHOP were determined by western blot to indicate ER stress. JPH2 knockdown resulted in greater expression of CHOP by 40% in cardiomyocytes (Figure 20). Ryanodine resulted in lower JPH2 knockdown-induced CHOP expression by 25% and 70% in neonatal cardiomyocytes (Figure 20).

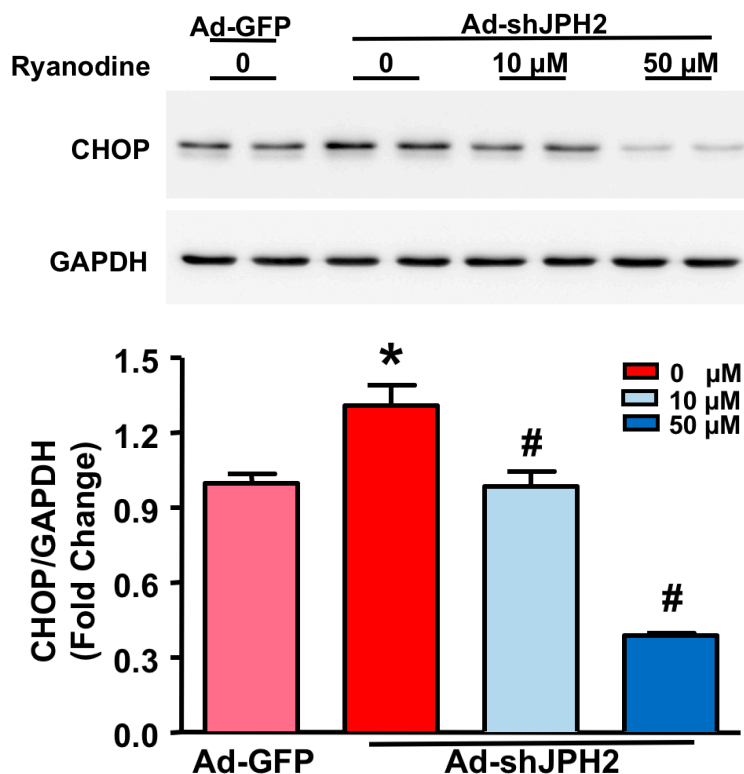


Figure 20: Inhibition of Ca^{2+} release from RyR2 reduces JPH2 knockdown-induced CHOP protein expression in neonatal mouse cardiomyocytes.

Neonatal mouse cardiomyocytes were isolated and cultured for 24 hours. After infection with Ad-shJPH2 or Ad-GFP with or without ryanodine incubation for 24 hours, the protein levels of CHOP were analyzed by western blot. GAPDH was used as a loading control. Upper panel: a representative western blot for CHOP and GAPDH from 4 different cultures in duplicate. Lower panel: quantitation of the protein levels of CHOP relative to GAPDH. Data was mean \pm SD from 4 independent experiments and analyzed by two-way ANOVA followed by Newman-Keuls test. * $P < 0.05$ versus Ad-GFP-0 μM ryanodine, # $P < 0.05$ versus Ad-shJPH2-0 μM ryanodine.

3.19 Inhibition of Ca^{2+} release from RyR2 reduces palmitate-induced apoptosis in cultured neonatal mouse cardiomyocytes

Since inhibition of Ca^{2+} release from RyR2 by ryanodine reduced palmitate-induced ER stress in cardiomyocytes, we next investigated if ryanodine decreased palmitate-induced apoptosis. Neonatal mouse cardiomyocytes were incubated with 800 μM OA or PA for 48 hours. At the same time, the cardiomyocytes were treated with or without 50 μM ryanodine. Caspase-3 activity was detected to indicate apoptosis in neonatal cardiomyocytes. PA incubation resulted in greater caspase-3 activity by 80% in cardiomyocytes compared to OA group. Ryanodine resulted in lower palmitate-induced caspase-3 activity by 30% in neonatal cardiomyocytes (Figure 21). This result demonstrated that inhibition of Ca^{2+} release from RyR2 reduces palmitate-induced apoptosis in cardiomyocytes.

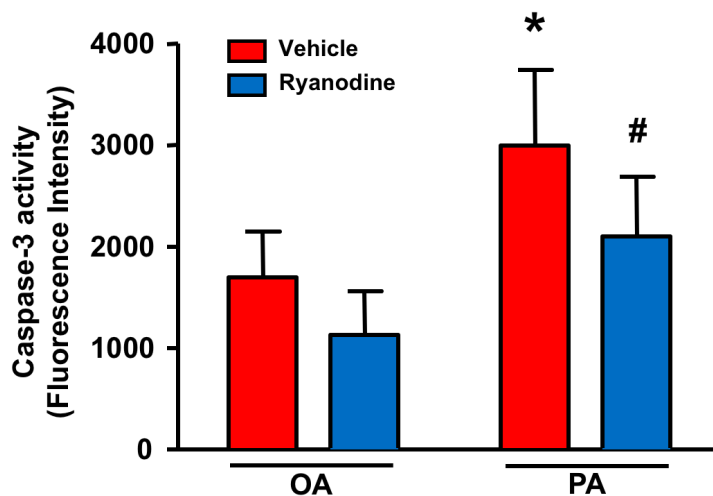


Figure 21: Inhibition of Ca^{2+} release from RyR2 reduces palmitate-induced caspase-3 activity in neonatal mouse cardiomyocytes.

Neonatal mouse cardiomyocytes were isolated and cultured for 24 hours. After incubation with oleate (OA) or palmitate (PA) with or without ryanodine treatment for 48 hours, caspase-3 activity was analyzed in neonatal mouse cardiomyocytes. Data was mean \pm SD from 8 independent experiments and analyzed by two-way ANOVA followed by Newman-Keuls test. * $P < 0.05$ versus OA-Vehicle, # $P < 0.05$ versus PA-Vehicle.

3.20 Ryanodine reduces palmitate-induced Ca^{2+} release in cultured neonatal mouse cardiomyocytes

Since disruption of Ca^{2+} homeostasis contributed to ER stress and apoptosis in cardiomyocytes (76), we next determined the cytoplasmic free Ca^{2+} level to further investigate if Ca^{2+} imbalance participated in palmitate-induced cardiomyocyte injury. Neonatal mouse cardiomyocytes were incubated with 800 μM OA or PA for 48 hours. At the same time, the cardiomyocytes were treated with or without 50 μM ryanodine. Fura-2 AM was used to stain cytoplasmic free Ca^{2+} in cardiomyocytes. Ryanodine was administered to inhibit Ca^{2+} release from RyR2 in cardiomyocytes. PA incubation resulted in greater cytoplasmic free Ca^{2+} by 160% in cardiomyocytes compared to OA group. Ryanodine resulted in lower palmitate-induced cytoplasmic free Ca^{2+} by 50% in neonatal cardiomyocytes (Figure 22). This result demonstrated that palmitate incubation induces excessive Ca^{2+} release and ryanodine reduces palmitate-induced Ca^{2+} release in cardiomyocytes.

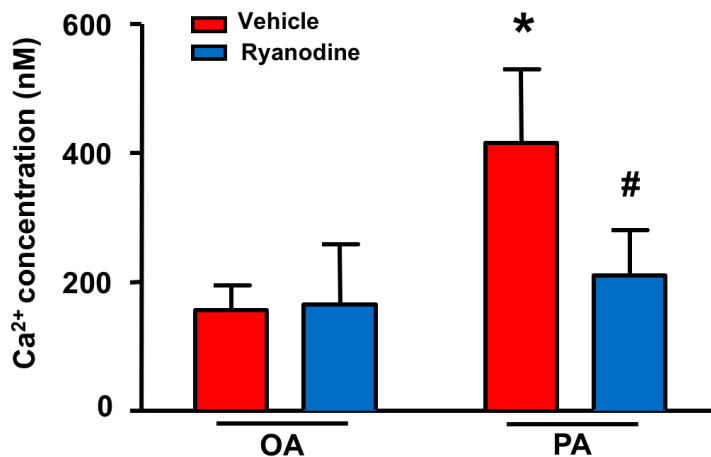


Figure 22 Ryanodine reduces palmitate-induced Ca²⁺ release in neonatal mouse cardiomyocytes.

Neonatal mouse cardiomyocytes were isolated and cultured for 24 hours. After incubation with oleate (OA) or palmitate (PA) with or without ryanodine treatment for 48 hours, cytoplasmic free Ca²⁺ was analyzed in neonatal mouse cardiomyocytes. Data was mean \pm SD from 4 independent experiments and analyzed by two-way ANOVA followed by Newman-Keuls test. * P < 0.05 versus OA-Vehicle, # P < 0.05 versus PA-Vehicle.

3.21 JPH2 over-expression attenuates palmitate-induced Ca^{2+} release in cultured neonatal mouse cardiomyocytes

As mentioned before, JPH2 protected cardiomyocytes against palmitate-induced injury by preventing ER stress and subsequent apoptosis. Palmitate incubation increased cytoplasmic free Ca^{2+} relative to oleate, contributing to ER stress and apoptosis in cardiomyocytes. We hypothesized that JPH2 protected cardiomyocytes against palmitate-induced ER stress and apoptosis through preventing excessive Ca^{2+} release in cardiomyocytes. To demonstrate this, neonatal mouse cardiomyocytes were infected with Ad-JPH2 (40 PFU/cell) or Ad-HA (40 PFU/cell) for 24 hours and then treated with 800 μM PA or OA for another 24 hours. Fura-2 AM was used to stain cytoplasmic free Ca^{2+} in cardiomyocytes. PA incubation resulted in greater cytoplasmic free Ca^{2+} by 100% in cardiomyocytes compared to OA group. JPH2 over-expression resulted in lower palmitate-induced cytoplasmic free Ca^{2+} by 45% in neonatal cardiomyocytes (Figure 23). This result demonstrated that JPH2 over-expression attenuates palmitate-induced Ca^{2+} release in cardiomyocytes.

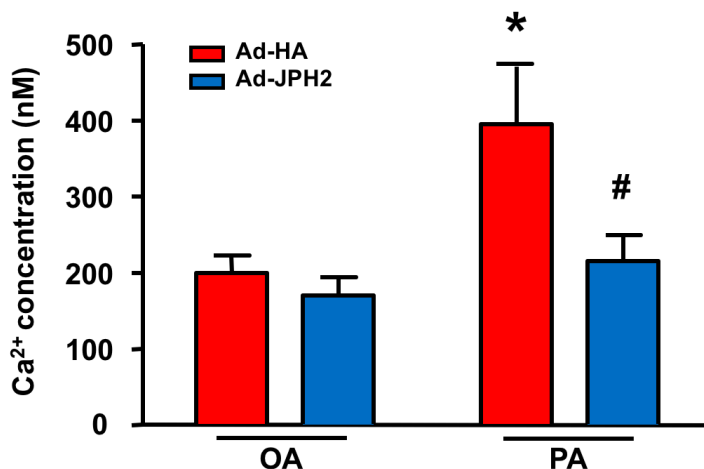


Figure 23 JPH2 over-expression attenuates palmitate-induced Ca²⁺ release in neonatal mouse cardiomyocytes.

Neonatal mouse cardiomyocytes were isolated and cultured for 24 hours. After infection with Ad-JPH2 or Ad-HA, together with incubation with oleate (OA) or palmitate (PA) for 48 hours, cytoplasmic free Ca²⁺ was analyzed in neonatal mouse cardiomyocytes. Data was mean \pm SD from 4 independent experiments and analyzed by two-way ANOVA followed by Newman-Keuls test. * P < 0.05 versus OA-Ad-HA, # P < 0.05 versus PA-Ad-HA.

Chapter 4

4 Discussion, Limitations and Future Directions

4.1 Discussion

The major findings of this study are that silencing of JPH2 enhances, whereas over-expression of JPH2 reduces palmitate-induced apoptosis in cardiomyocytes. Also, over-expression of JPH2 attenuates palmitate-induced CHOP expression and apoptosis while deletion of CHOP prevents apoptosis in palmitate-stimulated cardiomyocytes. Furthermore, over-expression of JPH2 lowers the levels of cytosolic free Ca^{2+} and blockage of Ca^{2+} release from RyR2 with ryanodine reduces the levels of CHOP protein and inhibits apoptosis in palmitate-stimulated cardiomyocytes. Additionally, silencing of JPH2 sufficiently induces CHOP expression, increases cytosolic free Ca^{2+} and elicits apoptosis in cardiomyocytes. These effects of JPH2 knockdown are prevented by CHOP deletion and blockage of Ca^{2+} release from RyR2. Thus, our study reveals a novel protection of JPH2 against palmitate-induced apoptosis in cardiomyocytes.

4.1.1 Palmitate-mediated down-regulation of JPH2 in cardiomyocytes

A reduction of JPH2 protein has been reported in human diseased hearts including dilated cardiomyopathy, hypertrophy and heart failure (36, 43, 169, 170). JPH2 down-regulation has also been found in mouse models of heart diseases (53, 58, 171). Studies from our lab showed that the protein levels of JPH2 were decreased in high fat diet-fed mouse hearts and that in cultured neonatal cardiomyocytes and incubation with palmitate led to a reduction of JPH2 protein levels when compared to oleate (2). Consistent with this prior report, the present study also shows that palmitate incubation reduces the protein levels of

JPH2 in cultured neonatal cardiomyocytes when compared to oleate. These studies suggest that JPH2 expression may be altered in cardiomyocytes with metabolic disorders. Although palmitate represents an important saturated free fatty acid in western diets, which contributes to cardiac lipotoxic injury in metabolic disorders (28), there are other important dietary saturated free fatty acids such as myristic acid and stearic acid. It remains to be determined if these other saturated free fatty acids also induce down-regulation of JPH2 in cardiomyocytes. In addition, it is unknown whether high glucose plays a role in the regulation of JPH2 in cardiomyocytes. Currently, we do not know how palmitate causes down-regulation of JPH2 protein in cardiomyocytes. A prior study showed that inhibition of calpain increased the protein levels of JPH2 in palmitate-stimulated cardiomyocytes and high fat diet-fed mouse hearts (2), underscoring an important role of calpain activation in down-regulation of JPH2. Indeed, it has been reported that calpain directly cleaves JPH2 protein at the site of R565T in the C-terminal of JPH2 (172), leading to down-regulation of JPH2 during myocardial ischemia/reperfusion injury. In addition to calpain activation, alternative mechanisms have also been reported to be contributed to dysregulation of JPH2 in the heart under stress. First, it is shown that up-regulated miR-24 is correlated with JPH2 down-regulation in human diseased hearts and that inhibition of miR-24 restores JPH2 expression in mouse model of cardiac hypertrophy (48). Mechanistic study reveals that miR-24 targets and represses JPH2 protein translation through a binding site in the 3'-terminal of JPH2 mRNA (48). Second, it is reported that JPH2 is the target of miR-34a in diseased hearts (173). Third, a very recent study shows that MMP-2 directly cleaves and down-regulates JPH2 protein in cardiomyocytes following ischemia/reperfusion injury (57). We currently do not know whether these alternative mechanisms are involved in the

palmitate-induced down-regulation of JPH2 protein in cardiomyocytes, but it is possible that they may contribute to JPH2 protein down-regulation as miR-24, miR-34a and MMP-2 have been reported to increase in hearts with metabolic disorders (48, 51, 57, 173).

It is important to point out that the mechanisms mentioned above account for post-transcriptional and post-translational regulation. The transcription regulatory mechanism responsible for JPH2 mRNA expression has never been demonstrated. It is currently unknown whether the transcriptional mechanism is involved; however, it merits further investigation for clarification.

4.1.2 Novel cardiac protection of JPH2 against palmitate-induced apoptosis

JPH2 is an important structural protein in forming junctional membrane complexes (JMCs), essential for excitation-contraction coupling within cardiomyocytes (36). It is clear that JPH2 is important in anchoring junctional sarcoplasmic reticulum and transverse-tubule (T-tubule) membrane invaginations (34). Additionally, JPH2 is also necessary for the development of postnatal T-tubules in mammals (174). Recent studies have found that JPH2 plays a critical role in maintaining the complex JMC architecture and stabilizing local ion channels in mature cardiomyocytes (39). Loss of JPH2's function by mutations or down-regulation of its protein expression is associated with hypertrophic cardiomyopathy, arrhythmias, and the progression of heart failure (31, 35, 43).

The present study reveals an unrecognized role of JPH2 in protecting cardiomyocytes against palmitate-induced apoptosis. Several lines of evidences support this conclusion. First, a reduction of JPH2 protein is associated with occurrence of apoptosis in cardiomyocytes in response to palmitate when compared to oleate. Second, over-expression of JPH2 attenuates whereas silencing of JPH2 enhances palmitate-induced

apoptosis in cardiomyocytes. Third, silencing of JPH2 induces apoptosis in cardiomyocytes. This also suggests that JPH2 is necessary for cardiomyocyte survival. Thus, this study provides additional evidence in support of cardio-protection by JPH2. Our findings together with a previous report (2) suggest that targeting JPH2 may be an effective strategy to prevent/treat cardiac injury under stress.

4.1.3 JPH2 prevention of ER stress in cardiomyocytes during lipotoxicity

Palmitate has been linked to ER stress contributing to cell death via apoptosis in cardiomyocytes (27, 28). In line with this, the present study shows that palmitate induces CHOP protein expression in cardiomyocytes, indicative of ER stress. Interestingly, the induction of CHOP is associated with a reduction of JPH2 in palmitate-stimulated cardiomyocytes. Importantly, over-expression of JPH2 prevents palmitate-induced CHOP expression in cardiomyocytes. These findings suggest that JPH2 suppresses the induction of ER stress in palmitate-stimulated cardiomyocytes. This is further supported by additional experimental evidence which shows that silencing of JPH2 induces CHOP expression in cardiomyocytes.

Since our present data has shown that JPH2 protects cardiomyocytes against palmitate-induced apoptosis, it is reasonable to suspect that the role of JPH2 is mediated through prevention of CHOP induction. Indeed, deletion of CHOP attenuates both palmitate- and JPH2 knockdown-induced apoptosis in cardiomyocytes. Thus, we argue that palmitate leads to a reduction of JPH2, which mediates CHOP induction, leading to apoptosis in cardiomyocytes.

However, we currently do not know the mechanisms by which a reduction of JPH2 induces ER stress or CHOP expression in cardiomyocytes. It is well known that ER stress can be

caused by oxidative stress, ischemia, disturbance of Ca^{2+} homeostasis etc. (77, 175-179). We know that JPH2 keeps proper Ca^{2+} -induced Ca^{2+} release in cardiomyocytes. Of note, recent studies have demonstrated a role of JPH2 in stabilizing RyR2 (43, 180), which gates the release of Ca^{2+} from ER/SR into the cytosol, suggesting that JPH2 may function as a brake on Ca^{2+} release from RyR2 as the loss of JPH2 results in aberrant Ca^{2+} leakage from the SR through RyR2 (181). Thus, it is most likely that a reduction of JPH2 may lead to more Ca^{2+} release from RyR2 into the cytosol, resulting in an elevation of free Ca^{2+} , which contributes to apoptosis in palmitate-stimulated cardiomyocytes. In line with this, we shows that palmitate or silencing of JPH2 elevates the levels of free Ca^{2+} in the cytosol, and that over-expression of JPH2 decreases the levels of free Ca^{2+} in the cytosol in palmitate-stimulated cardiomyocytes. Furthermore, blocking Ca^{2+} release from RyR2 attenuates CHOP expression and apoptosis induced by palmitate and silencing of JPH2 in cardiomyocytes. Nevertheless, it remains to be determined how JPH2 stabilizes RyR2 in controlling Ca^{2+} release in cardiomyocytes.

On the other hand, an elevation of cytosolic Ca^{2+} may result from dysfunction of the sarco/endoplasmic reticulum Ca^{2+} ATPase (SERCA) pump and/or Na^+ - Ca^{2+} exchanger (NCX) as the former pumps Ca^{2+} into ER/SR and the latter exports Ca^{2+} outside of cardiomyocytes (75). Both are compromised in cardiomyocytes during metabolic disorders (181-185). Interestingly, studies have shown that JPH2 regulates NCX participating in regulation of Ca^{2+} homeostasis in cardiomyocytes (181). Future studies are needed to determine whether this is also operative in palmitate-stimulated cardiomyocytes.

4.1.4 Concluding remarks

We have provided evidence that demonstrates an unrecognized role of JPH2 in cardiomyocytes in prevention of apoptosis induced by palmitate. This new role of JPH2 may be mediated through attenuation of Ca^{2+} release from RyR2 and subsequent CHOP expression (also see Figure 24). Given that palmitate has been widely used to induce lipotoxicity in cardiomyocytes, targeting JPH2 may represent a new therapeutic strategy to reduce cardiac injury in lipotoxicity.

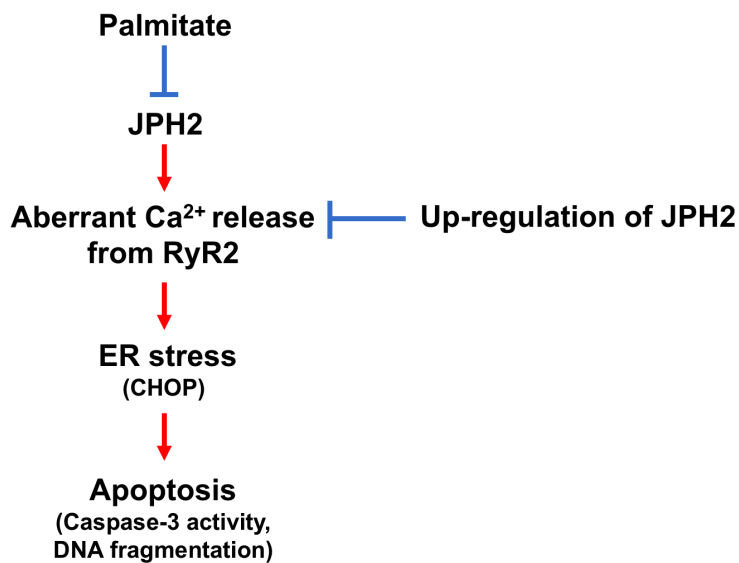


Figure 24: Summary of findings.

4.2 Limitations and future directions

We used oleate as a control for palmitate. It is better to include the non-treated control and investigate whether oleate plays any roles in cardiomyocytes. However, previous studies have shown that oleate does not have any effects on apoptosis and junctophilin-2 expression in cardiomyocytes.

The present study is focused on isolated neonatal mouse cardiomyocytes. However, the role of JPH2 in lipotoxicity induced cell injury in vivo remains unknown. High fat diet mouse model will be established to investigate whether JPH2 plays a protective role in vivo.

Although our recent study showed that deletion of calpain attenuated the reduction of JPH2 in palmitate-stimulated cardiomyocytes and mice fed with HFD, we can not exclude other mechanisms contributing to JPH2 down-regulation such as through miR-24, miR-34a and MMP2, which may be examined in future studies.

Future studies are also needed to determine how JPH2 modulates Ca^{2+} release from RyR2 in cardiomyocytes. Prior studies have shown that JPH2 may be implicated in RyR2 stability. Thus, we will investigate the molecular basis of JPH2 stabilizing RyR2 in cardiomyocytes. On the other hand, oxidative damage to SERCA may also contribute to cytosolic Ca^{2+} overload in cardiomyocytes (182), which merits further investigation.

References

1. K. D'Souza, C. Nzirorera, P. C. Kienesberger, Lipid metabolism and signaling in cardiac lipotoxicity. *Biochim Biophys Acta* **1861**, 1513-1524 (2016).
2. S. Li *et al.*, Disruption of calpain reduces lipotoxicity-induced cardiac injury by preventing endoplasmic reticulum stress. *Biochim Biophys Acta* **1862**, 2023-2033 (2016).
3. J. R. Goldenberg *et al.*, Preservation of Acyl Coenzyme A Attenuates Pathological and Metabolic Cardiac Remodeling Through Selective Lipid Trafficking. *Circulation* **139**, 2765-2777 (2019).
4. G. D. Lopaschuk, J. R. Ussher, C. D. Folmes, J. S. Jaswal, W. C. Stanley, Myocardial fatty acid metabolism in health and disease. *Physiol Rev* **90**, 207-258 (2010).
5. W. C. Stanley, F. A. Recchia, G. D. Lopaschuk, Myocardial substrate metabolism in the normal and failing heart. *Physiol Rev* **85**, 1093-1129 (2005).
6. I. Zlobine, K. Gopal, J. R. Ussher, Lipotoxicity in obesity and diabetes-related cardiac dysfunction. *Biochim Biophys Acta* **1861**, 1555-1568 (2016).
7. G. D. Lopaschuk, C. D. Folmes, W. C. Stanley, Cardiac energy metabolism in obesity. *Circ Res* **101**, 335-347 (2007).
8. D. B. Savage, K. F. Petersen, G. I. Shulman, Disordered lipid metabolism and the pathogenesis of insulin resistance. *Physiol Rev* **87**, 507-520 (2007).
9. H. Taegtmeyer, P. McNulty, M. E. Young, Adaptation and maladaptation of the heart in diabetes: Part I: general concepts. *Circulation* **105**, 1727-1733 (2002).
10. M. E. Young, P. McNulty, H. Taegtmeyer, Adaptation and maladaptation of the heart in diabetes: Part II: potential mechanisms. *Circulation* **105**, 1861-1870 (2002).
11. K. Drosatos, P. C. Schulze, Cardiac lipotoxicity: molecular pathways and therapeutic implications. *Curr Heart Fail Rep* **10**, 109-121 (2013).
12. J. R. Ussher, The role of cardiac lipotoxicity in the pathogenesis of diabetic cardiomyopathy. *Expert Rev Cardiovasc Ther* **12**, 345-358 (2014).
13. D. M. Muoio, P. D. Neuffer, Lipid-induced mitochondrial stress and insulin action in muscle. *Cell Metab* **15**, 595-605 (2012).
14. H. Lin, X. Su, B. He, Protein lysine acylation and cysteine succination by intermediates of energy metabolism. *ACS Chem Biol* **7**, 947-960 (2012).
15. L. H. Chamberlain, M. J. Shipston, The physiology of protein S-acylation. *Physiol Rev* **95**, 341-376 (2015).
16. W. L. Holland *et al.*, Inhibition of ceramide synthesis ameliorates glucocorticoid-, saturated-fat-, and obesity-induced insulin resistance. *Cell Metab* **5**, 167-179 (2007).
17. J. R. Ussher *et al.*, Inhibition of de novo ceramide synthesis reverses diet-induced insulin resistance and enhances whole-body oxygen consumption. *Diabetes* **59**, 2453-2464 (2010).
18. L. Pickersgill, G. J. Litherland, A. S. Greenberg, M. Walker, S. J. Yeaman, Key role for ceramides in mediating insulin resistance in human muscle cells. *J Biol Chem* **282**, 12583-12589 (2007).

19. J. Y. Xia *et al.*, Targeted Induction of Ceramide Degradation Leads to Improved Systemic Metabolism and Reduced Hepatic Steatosis. *Cell Metab* **22**, 266-278 (2015).
20. R. W. Ledeen, G. Wu, Nuclear sphingolipids: metabolism and signaling. *J Lipid Res* **49**, 1176-1186 (2008).
21. T. D. Mullen, L. M. Obeid, Ceramide and apoptosis: exploring the enigmatic connections between sphingolipid metabolism and programmed cell death. *Anticancer Agents Med Chem* **12**, 340-363 (2012).
22. H. C. Chiu *et al.*, A novel mouse model of lipotoxic cardiomyopathy. *J Clin Invest* **107**, 813-822 (2001).
23. L. Liu *et al.*, DGAT1 expression increases heart triglyceride content but ameliorates lipotoxicity. *J Biol Chem* **284**, 36312-36323 (2009).
24. M. Park *et al.*, APPL1 transgenic mice are protected from high-fat diet-induced cardiac dysfunction. *Am J Physiol Endocrinol Metab* **305**, E795-804 (2013).
25. G. Carta, E. Murru, S. Banni, C. Manca, Palmitic Acid: Physiological Role, Metabolism and Nutritional Implications. *Front Physiol* **8**, 902 (2017).
26. Diet, nutrition and the prevention of chronic diseases. *World Health Organ Tech Rep Ser* **916**, i-viii, 1-149, backcover (2003).
27. K. Tsushima *et al.*, Mitochondrial Reactive Oxygen Species in Lipotoxic Hearts Induce Post-Translational Modifications of AKAP121, DRP1, and OPA1 That Promote Mitochondrial Fission. *Circ Res* **122**, 58-73 (2018).
28. A. Sakamoto *et al.*, Eicosapentaenoic acid ameliorates palmitate-induced lipotoxicity via the AMP kinase/dynamin-related protein-1 signaling pathway in differentiated H9c2 myocytes. *Exp Cell Res* **351**, 109-120 (2017).
29. T. Haffar, F. A. Bérubé-Simard, N. Boussette, Cardiomyocyte lipotoxicity is mediated by Il-6 and causes down-regulation of PPARs. *Biochem Biophys Res Commun* **459**, 54-59 (2015).
30. H. Takeshima, S. Komazaki, M. Nishi, M. Iino, K. Kangawa, Junctophilins: a novel family of junctional membrane complex proteins. *Mol Cell* **6**, 11-22 (2000).
31. A. Garbino, X. H. Wehrens, Emerging role of junctophilin-2 as a regulator of calcium handling in the heart. *Acta Pharmacol Sin* **31**, 1019-1021 (2010).
32. M. Nishi, H. Sakagami, S. Komazaki, H. Kondo, H. Takeshima, Coexpression of junctophilin type 3 and type 4 in brain. *Brain Res Mol Brain Res* **118**, 102-110 (2003).
33. H. Takeshima, M. Hoshijima, L. S. Song, Ca²⁺ microdomains organized by junctophilins. *Cell Calcium* **58**, 349-356 (2015).
34. B. Chen *et al.*, Critical roles of junctophilin-2 in T-tubule and excitation-contraction coupling maturation during postnatal development. *Cardiovasc Res* **100**, 54-62 (2013).
35. J. O. Reynolds *et al.*, Junctophilin-2 is necessary for T-tubule maturation during mouse heart development. *Cardiovasc Res* **100**, 44-53 (2013).
36. D. L. Beavers, A. P. Landstrom, D. Y. Chiang, X. H. Wehrens, Emerging roles of junctophilin-2 in the heart and implications for cardiac diseases. *Cardiovasc Res* **103**, 198-205 (2014).
37. A. Guo *et al.*, E-C coupling structural protein junctophilin-2 encodes a stress-adaptive transcription regulator. *Science* **362**, (2018).

38. A. Guo, C. Zhang, S. Wei, B. Chen, L. S. Song, Emerging mechanisms of T-tubule remodelling in heart failure. *Cardiovasc Res* **98**, 204-215 (2013).
39. R. J. van Oort *et al.*, Disrupted junctional membrane complexes and hyperactive ryanodine receptors after acute junctophilin knockdown in mice. *Circulation* **123**, 979-988 (2011).
40. S. Wei *et al.*, T-tubule remodeling during transition from hypertrophy to heart failure. *Circ Res* **107**, 520-531 (2010).
41. Y. P. Xie *et al.*, Sildenafil prevents and reverses transverse-tubule remodeling and Ca(2+) handling dysfunction in right ventricle failure induced by pulmonary artery hypertension. *Hypertension* **59**, 355-362 (2012).
42. H. D. Wu *et al.*, Ultrastructural remodelling of Ca(2+) signalling apparatus in failing heart cells. *Cardiovasc Res* **95**, 430-438 (2012).
43. D. L. Beavers *et al.*, Mutation E169K in junctophilin-2 causes atrial fibrillation due to impaired RyR2 stabilization. *J Am Coll Cardiol* **62**, 2010-2019 (2013).
44. E. Wagner *et al.*, Stimulated emission depletion live-cell super-resolution imaging shows proliferative remodeling of T-tubule membrane structures after myocardial infarction. *Circ Res* **111**, 402-414 (2012).
45. D. Dobrev, N. Voigt, X. H. Wehrens, The ryanodine receptor channel as a molecular motif in atrial fibrillation: pathophysiological and therapeutic implications. *Cardiovasc Res* **89**, 734-743 (2011).
46. N. Voigt *et al.*, Enhanced sarcoplasmic reticulum Ca²⁺ leak and increased Na⁺-Ca²⁺ exchanger function underlie delayed afterdepolarizations in patients with chronic atrial fibrillation. *Circulation* **125**, 2059-2070 (2012).
47. R. Wakili, N. Voigt, S. Käähb, D. Dobrev, S. Nattel, Recent advances in the molecular pathophysiology of atrial fibrillation. *J Clin Invest* **121**, 2955-2968 (2011).
48. M. Xu *et al.*, Mir-24 regulates junctophilin-2 expression in cardiomyocytes. *Circ Res* **111**, 837-841 (2012).
49. E. van Rooij *et al.*, A signature pattern of stress-responsive microRNAs that can evoke cardiac hypertrophy and heart failure. *Proc Natl Acad Sci U S A* **103**, 18255-18260 (2006).
50. H. B. Zhang *et al.*, Ultrastructural uncoupling between T-tubules and sarcoplasmic reticulum in human heart failure. *Cardiovasc Res* **98**, 269-276 (2013).
51. R. C. Li *et al.*, In vivo suppression of microRNA-24 prevents the transition toward decompensated hypertrophy in aortic-constricted mice. *Circ Res* **112**, 601-605 (2013).
52. J. Hu *et al.*, RBFox2-miR-34a-Jph2 axis contributes to cardiac decompensation during heart failure. *Proceedings of the National Academy of Sciences* **116**, 6172-6180 (2019).
53. C. Y. Wu *et al.*, Calpain-dependent cleavage of junctophilin-2 and T-tubule remodeling in a mouse model of reversible heart failure. *J Am Heart Assoc* **3**, e000527 (2014).
54. M. Zatz, A. Starling, Calpains and disease. *N Engl J Med* **352**, 2413-2423 (2005).

55. C. Patterson, A. L. Portbury, J. C. Schisler, M. S. Willis, Tear me down: role of calpain in the development of cardiac ventricular hypertrophy. *Circ Res* **109**, 453-462 (2011).
56. R. M. Murphy *et al.*, Ca²⁺-dependent proteolysis of junctophilin-1 and junctophilin-2 in skeletal and cardiac muscle. *J Physiol* **591**, 719-729 (2013).
57. B. Y. H. Chan *et al.*, Junctophilin-2 is a target of matrix metalloproteinase-2 in myocardial ischemia-reperfusion injury. *Basic Res Cardiol* **114**, 42 (2019).
58. C. Zhang *et al.*, Microtubule-mediated defects in junctophilin-2 trafficking contribute to myocyte transverse-tubule remodeling and Ca²⁺ handling dysfunction in heart failure. *Circulation* **129**, 1742-1750 (2014).
59. G. Cooper, Cytoskeletal networks and the regulation of cardiac contractility: microtubules, hypertrophy, and cardiac dysfunction. *Am J Physiol Heart Circ Physiol* **291**, H1003-1014 (2006).
60. S. Doroudgar, C. C. Glembotski, New concepts of endoplasmic reticulum function in the heart: programmed to conserve. *J Mol Cell Cardiol* **55**, 85-91 (2013).
61. T. A. Lagace, N. D. Ridgway, The role of phospholipids in the biological activity and structure of the endoplasmic reticulum. *Biochim Biophys Acta* **1833**, 2499-2510 (2013).
62. J. Groenendyk, P. K. Sreenivasaiah, D. H. Kim, L. B. Agellon, M. Michalak, Biology of endoplasmic reticulum stress in the heart. *Circ Res* **107**, 1185-1197 (2010).
63. C. Hetz, The unfolded protein response: controlling cell fate decisions under ER stress and beyond. *Nat Rev Mol Cell Biol* **13**, 89-102 (2012).
64. L. Ellgaard, A. Helenius, Quality control in the endoplasmic reticulum. *Nat Rev Mol Cell Biol* **4**, 181-191 (2003).
65. M. Schröder, R. J. Kaufman, The mammalian unfolded protein response. *Annu Rev Biochem* **74**, 739-789 (2005).
66. C. Hetz, F. Martinon, D. Rodriguez, L. H. Glimcher, The unfolded protein response: integrating stress signals through the stress sensor IRE1 α . *Physiol Rev* **91**, 1219-1243 (2011).
67. U. Woehlbier, C. Hetz, Modulating stress responses by the UPRosome: a matter of life and death. *Trends Biochem Sci* **36**, 329-337 (2011).
68. E. Sozen, B. Karademir, N. K. Ozer, Basic mechanisms in endoplasmic reticulum stress and relation to cardiovascular diseases. *Free Radic Biol Med* **78**, 30-41 (2015).
69. J. Grootjans, A. Kaser, R. J. Kaufman, R. S. Blumberg, The unfolded protein response in immunity and inflammation. *Nat Rev Immunol* **16**, 469-484 (2016).
70. C. Hetz, E. Chevet, S. A. Oakes, Proteostasis control by the unfolded protein response. *Nat Cell Biol* **17**, 829-838 (2015).
71. C. Hetz, E. Chevet, H. P. Harding, Targeting the unfolded protein response in disease. *Nat Rev Drug Discov* **12**, 703-719 (2013).
72. R. J. Kaufman *et al.*, The unfolded protein response in nutrient sensing and differentiation. *Nat Rev Mol Cell Biol* **3**, 411-421 (2002).
73. D. Ron, Translational control in the endoplasmic reticulum stress response. *J Clin Invest* **110**, 1383-1388 (2002).

74. U. Ozcan *et al.*, Endoplasmic reticulum stress links obesity, insulin action, and type 2 diabetes. *Science* **306**, 457-461 (2004).
75. A. Fabiato, Calcium-induced release of calcium from the cardiac sarcoplasmic reticulum. *Am J Physiol* **245**, C1-14 (1983).
76. C. Ahn, B. S. An, E. B. Jeung, Streptozotocin induces endoplasmic reticulum stress and apoptosis via disruption of calcium homeostasis in mouse pancreas. *Mol Cell Endocrinol* **412**, 302-308 (2015).
77. S. Xu *et al.*, RCN1 suppresses ER stress-induced apoptosis via calcium homeostasis and PERK-CHOP signaling. *Oncogenesis* **6**, e304 (2017).
78. D. S. Luciani *et al.*, Roles of IP3R and RyR Ca²⁺ channels in endoplasmic reticulum stress and beta-cell death. *Diabetes* **58**, 422-432 (2009).
79. I. Tabas, D. Ron, Integrating the mechanisms of apoptosis induced by endoplasmic reticulum stress. *Nat Cell Biol* **13**, 184-190 (2011).
80. S. Oyadomari, M. Mori, Roles of CHOP/GADD153 in endoplasmic reticulum stress. *Cell Death Differ* **11**, 381-389 (2004).
81. D. Ron, J. F. Habener, CHOP, a novel developmentally regulated nuclear protein that dimerizes with transcription factors C/EBP and LAP and functions as a dominant-negative inhibitor of gene transcription. *Genes Dev* **6**, 439-453 (1992).
82. H. Zinszner *et al.*, CHOP is implicated in programmed cell death in response to impaired function of the endoplasmic reticulum. *Genes Dev* **12**, 982-995 (1998).
83. K. Okada *et al.*, Prolonged endoplasmic reticulum stress in hypertrophic and failing heart after aortic constriction: possible contribution of endoplasmic reticulum stress to cardiac myocyte apoptosis. *Circulation* **110**, 705-712 (2004).
84. T. Okada, H. Yoshida, R. Akazawa, M. Negishi, K. Mori, Distinct roles of activating transcription factor 6 (ATF6) and double-stranded RNA-activated protein kinase-like endoplasmic reticulum kinase (PERK) in transcription during the mammalian unfolded protein response. *Biochem J* **366**, 585-594 (2002).
85. K. D. McCullough, J. L. Martindale, L. O. Klotz, T. Y. Aw, N. J. Holbrook, Gadd153 sensitizes cells to endoplasmic reticulum stress by down-regulating Bcl2 and perturbing the cellular redox state. *Mol Cell Biol* **21**, 1249-1259 (2001).
86. T. Gotoh, M. Mori, [Regulation of apoptosis by molecular chaperones]. *Tanpakushitsu Kakusan Koso* **49**, 1010-1013 (2004).
87. A. X. Zhou, I. Tabas, The UPR in atherosclerosis. *Semin Immunopathol* **35**, 321-332 (2013).
88. C. W. Younce, A. Azfer, P. E. Kolattukudy, MCP-1 (monocyte chemotactic protein-1)-induced protein, a recently identified zinc finger protein, induces adipogenesis in 3T3-L1 pre-adipocytes without peroxisome proliferator-activated receptor gamma. *J Biol Chem* **284**, 27620-27628 (2009).
89. M. Bosma *et al.*, Sequestration of fatty acids in triglycerides prevents endoplasmic reticulum stress in an in vitro model of cardiomyocyte lipotoxicity. *Biochim Biophys Acta* **1841**, 1648-1655 (2014).
90. M. C. Maiuri, E. Zalckvar, A. Kimchi, G. Kroemer, Self-eating and self-killing: crosstalk between autophagy and apoptosis. *Nat Rev Mol Cell Biol* **8**, 741-752 (2007).

91. E. A. Slee, C. Adrain, S. J. Martin, Executioner caspase-3, -6, and -7 perform distinct, non-redundant roles during the demolition phase of apoptosis. *J Biol Chem* **276**, 7320-7326 (2001).
92. R. A. Schlegel, P. Williamson, Phosphatidylserine, a death knell. *Cell Death Differ* **8**, 551-563 (2001).
93. M. A. Savitskaya, G. E. Onishchenko, Mechanisms of Apoptosis. *Biochemistry (Mosc)* **80**, 1393-1405 (2015).
94. G. M. Cohen, Caspases: the executioners of apoptosis. *Biochem J* **326 (Pt 1)**, 1-16 (1997).
95. H. Wajant, The Fas signaling pathway: more than a paradigm. *Science* **296**, 1635-1636 (2002).
96. F. C. Kischkel *et al.*, Cytotoxicity-dependent APO-1 (Fas/CD95)-associated proteins form a death-inducing signaling complex (DISC) with the receptor. *EMBO J* **14**, 5579-5588 (1995).
97. E. Teringova, P. Tousek, Apoptosis in ischemic heart disease. *J Transl Med* **15**, 87 (2017).
98. X. Saelens *et al.*, Toxic proteins released from mitochondria in cell death. *Oncogene* **23**, 2861-2874 (2004).
99. M. M. Hill, C. Adrain, P. J. Duriez, E. M. Creagh, S. J. Martin, Analysis of the composition, assembly kinetics and activity of native Apaf-1 apoptosomes. *EMBO J* **23**, 2134-2145 (2004).
100. M. Schuler, D. R. Green, Mechanisms of p53-dependent apoptosis. *Biochem Soc Trans* **29**, 684-688 (2001).
101. N. Joza *et al.*, Essential role of the mitochondrial apoptosis-inducing factor in programmed cell death. *Nature* **410**, 549-554 (2001).
102. S. Cory, J. M. Adams, The Bcl2 family: regulators of the cellular life-or-death switch. *Nat Rev Cancer* **2**, 647-656 (2002).
103. M. C. Wei *et al.*, Proapoptotic BAX and BAK: a requisite gateway to mitochondrial dysfunction and death. *Science* **292**, 727-730 (2001).
104. S. K. Chiou, L. Rao, E. White, Bcl-2 blocks p53-dependent apoptosis. *Mol Cell Biol* **14**, 2556-2563 (1994).
105. P. F. Li, R. Dietz, R. von Harsdorf, p53 regulates mitochondrial membrane potential through reactive oxygen species and induces cytochrome c-independent apoptosis blocked by Bcl-2. *EMBO J* **18**, 6027-6036 (1999).
106. N. D. Marchenko, A. Zaika, U. M. Moll, Death signal-induced localization of p53 protein to mitochondria. A potential role in apoptotic signaling. *J Biol Chem* **275**, 16202-16212 (2000).
107. B. Yang *et al.*, Dioscin protects against coronary heart disease by reducing oxidative stress and inflammation via Sirt1/Nrf2 and p38 MAPK pathways. *Mol Med Rep* **18**, 973-980 (2018).
108. M. D. Esposti, The roles of Bid. *Apoptosis* **7**, 433-440 (2002).
109. A. Toth *et al.*, Endoplasmic reticulum stress as a novel therapeutic target in heart diseases. *Cardiovasc Hematol Disord Drug Targets* **7**, 205-218 (2007).
110. R. J. Kaufman, Orchestrating the unfolded protein response in health and disease. *J Clin Invest* **110**, 1389-1398 (2002).

111. F. Urano *et al.*, Coupling of stress in the ER to activation of JNK protein kinases by transmembrane protein kinase IRE1. *Science* **287**, 664-666 (2000).
112. J. J. Ventura *et al.*, Chemical genetic analysis of the time course of signal transduction by JNK. *Mol Cell* **21**, 701-710 (2006).
113. C. Hetz *et al.*, Proapoptotic BAX and BAK modulate the unfolded protein response by a direct interaction with IRE1alpha. *Science* **312**, 572-576 (2006).
114. T. Yoneda *et al.*, Activation of caspase-12, an endoplasmic reticulum (ER) resident caspase, through tumor necrosis factor receptor-associated factor 2-dependent mechanism in response to the ER stress. *J Biol Chem* **276**, 13935-13940 (2001).
115. D. Han *et al.*, IRE1alpha kinase activation modes control alternate endoribonuclease outputs to determine divergent cell fates. *Cell* **138**, 562-575 (2009).
116. H. Yoshida, T. Matsui, A. Yamamoto, T. Okada, K. Mori, XBP1 mRNA is induced by ATF6 and spliced by IRE1 in response to ER stress to produce a highly active transcription factor. *Cell* **107**, 881-891 (2001).
117. H. Y. Fu *et al.*, Ablation of C/EBP homologous protein attenuates endoplasmic reticulum-mediated apoptosis and cardiac dysfunction induced by pressure overload. *Circulation* **122**, 361-369 (2010).
118. H. Puthalakath *et al.*, ER stress triggers apoptosis by activating BH3-only protein Bim. *Cell* **129**, 1337-1349 (2007).
119. C. X. Santos, L. Y. Tanaka, J. Wosniak, F. R. Laurindo, Mechanisms and implications of reactive oxygen species generation during the unfolded protein response: roles of endoplasmic reticulum oxidoreductases, mitochondrial electron transport, and NADPH oxidase. *Antioxid Redox Signal* **11**, 2409-2427 (2009).
120. H. Tsukano *et al.*, The endoplasmic reticulum stress-C/EBP homologous protein pathway-mediated apoptosis in macrophages contributes to the instability of atherosclerotic plaques. *Arterioscler Thromb Vasc Biol* **30**, 1925-1932 (2010).
121. S. J. Marciniak *et al.*, CHOP induces death by promoting protein synthesis and oxidation in the stressed endoplasmic reticulum. *Genes Dev* **18**, 3066-3077 (2004).
122. G. Li *et al.*, Role of ERO1-alpha-mediated stimulation of inositol 1,4,5-triphosphate receptor activity in endoplasmic reticulum stress-induced apoptosis. *J Cell Biol* **186**, 783-792 (2009).
123. T. Nakagawa, J. Yuan, Cross-talk between two cysteine protease families. Activation of caspase-12 by calpain in apoptosis. *J Cell Biol* **150**, 887-894 (2000).
124. M. Chen *et al.*, Bid is cleaved by calpain to an active fragment in vitro and during myocardial ischemia/reperfusion. *J Biol Chem* **276**, 30724-30728 (2001).
125. D. T. Rutkowski *et al.*, Adaptation to ER stress is mediated by differential stabilities of pro-survival and pro-apoptotic mRNAs and proteins. *PLoS Biol* **4**, e374 (2006).
126. H. Toko *et al.*, ATF6 is important under both pathological and physiological states in the heart. *J Mol Cell Cardiol* **49**, 113-120 (2010).
127. G. C. Sparagna, D. L. Hickson-Bick, L. M. Buja, J. B. McMillin, A metabolic role for mitochondria in palmitate-induced cardiac myocyte apoptosis. *Am J Physiol Heart Circ Physiol* **279**, H2124-2132 (2000).

128. D. L. Hickson-Bick, L. M. Buja, J. B. McMillin, Palmitate-mediated alterations in the fatty acid metabolism of rat neonatal cardiac myocytes. *J Mol Cell Cardiol* **32**, 511-519 (2000).
129. N. M. Borradaile *et al.*, A critical role for eukaryotic elongation factor 1A-1 in lipotoxic cell death. *Mol Biol Cell* **17**, 770-778 (2006).
130. N. M. Borradaile *et al.*, Disruption of endoplasmic reticulum structure and integrity in lipotoxic cell death. *J Lipid Res* **47**, 2726-2737 (2006).
131. M. D. Turner, Fatty acyl CoA-mediated inhibition of endoplasmic reticulum assembly. *Biochim Biophys Acta* **1693**, 1-4 (2004).
132. K. C. Wollert, H. Drexler, Regulation of cardiac remodeling by nitric oxide: focus on cardiac myocyte hypertrophy and apoptosis. *Heart Fail Rev* **7**, 317-325 (2002).
133. E. Braunwald, M. R. Bristow, Congestive heart failure: fifty years of progress. *Circulation* **102**, IV14-23 (2000).
134. B. H. Lorell, B. A. Carabello, Left ventricular hypertrophy: pathogenesis, detection, and prognosis. *Circulation* **102**, 470-479 (2000).
135. D. Levy, R. J. Garrison, D. D. Savage, W. B. Kannel, W. P. Castelli, Prognostic implications of echocardiographically determined left ventricular mass in the Framingham Heart Study. *N Engl J Med* **322**, 1561-1566 (1990).
136. H. M. Krumholz, M. Larson, D. Levy, Prognosis of left ventricular geometric patterns in the Framingham Heart Study. *J Am Coll Cardiol* **25**, 879-884 (1995).
137. A. M. Segura, O. H. Frazier, L. M. Buja, Fibrosis and heart failure. *Heart Fail Rev* **19**, 173-185 (2014).
138. L. Lu *et al.*, Cardiac fibrosis in the ageing heart: Contributors and mechanisms. *Clin Exp Pharmacol Physiol* **44 Suppl 1**, 55-63 (2017).
139. J. K. Mouw, G. Ou, V. M. Weaver, Extracellular matrix assembly: a multiscale deconstruction. *Nat Rev Mol Cell Biol* **15**, 771-785 (2014).
140. C. Bonnans, J. Chou, Z. Werb, Remodelling the extracellular matrix in development and disease. *Nat Rev Mol Cell Biol* **15**, 786-801 (2014).
141. R. Kakkar, R. T. Lee, Intramyocardial fibroblast myocyte communication. *Circ Res* **106**, 47-57 (2010).
142. M. A. Bogoyevitch *et al.*, Endothelin-1 and fibroblast growth factors stimulate the mitogen-activated protein kinase signaling cascade in cardiac myocytes. The potential role of the cascade in the integration of two signaling pathways leading to myocyte hypertrophy. *J Biol Chem* **269**, 1110-1119 (1994).
143. D. Kaye *et al.*, Role of transiently altered sarcolemmal membrane permeability and basic fibroblast growth factor release in the hypertrophic response of adult rat ventricular myocytes to increased mechanical activity in vitro. *J Clin Invest* **97**, 281-291 (1996).
144. C. Pellieux *et al.*, Dilated cardiomyopathy and impaired cardiac hypertrophic response to angiotensin II in mice lacking FGF-2. *J Clin Invest* **108**, 1843-1851 (2001).
145. J. A. Virag *et al.*, Fibroblast growth factor-2 regulates myocardial infarct repair: effects on cell proliferation, scar contraction, and ventricular function. *Am J Pathol* **171**, 1431-1440 (2007).

146. S. L. House *et al.*, Fibroblast Growth Factor 2 Mediates Isoproterenol-induced Cardiac Hypertrophy through Activation of the Extracellular Regulated Kinase. *Mol Cell Pharmacol* **2**, 143-154 (2010).
147. F. Ma *et al.*, Macrophage-stimulated cardiac fibroblast production of IL-6 is essential for TGF β /Smad activation and cardiac fibrosis induced by angiotensin II. *PLoS One* **7**, e35144 (2012).
148. G. C. Meléndez *et al.*, Interleukin 6 mediates myocardial fibrosis, concentric hypertrophy, and diastolic dysfunction in rats. *Hypertension* **56**, 225-231 (2010).
149. B. C. Bernardo, K. L. Weeks, L. Pretorius, J. R. McMullen, Molecular distinction between physiological and pathological cardiac hypertrophy: experimental findings and therapeutic strategies. *Pharmacol Ther* **128**, 191-227 (2010).
150. K. T. Weber, C. G. Brilla, Pathological hypertrophy and cardiac interstitium. Fibrosis and renin-angiotensin-aldosterone system. *Circulation* **83**, 1849-1865 (1991).
151. P. Kong, P. Christia, N. G. Frangogiannis, The pathogenesis of cardiac fibrosis. *Cell Mol Life Sci* **71**, 549-574 (2014).
152. I. Kehat, J. D. Molkentin, Molecular pathways underlying cardiac remodeling during pathophysiological stimulation. *Circulation* **122**, 2727-2735 (2010).
153. F. G. Spinale, Myocardial matrix remodeling and the matrix metalloproteinases: influence on cardiac form and function. *Physiol Rev* **87**, 1285-1342 (2007).
154. R. D. Brown, S. K. Ambler, M. D. Mitchell, C. S. Long, The cardiac fibroblast: therapeutic target in myocardial remodeling and failure. *Annu Rev Pharmacol Toxicol* **45**, 657-687 (2005).
155. S. Verheule *et al.*, Increased vulnerability to atrial fibrillation in transgenic mice with selective atrial fibrosis caused by overexpression of TGF-beta1. *Circ Res* **94**, 1458-1465 (2004).
156. T. H. Everett, J. E. Olgin, Atrial fibrosis and the mechanisms of atrial fibrillation. *Heart Rhythm* **4**, S24-27 (2007).
157. A. Malgaroli, D. Milani, J. Meldolesi, T. Pozzan, Fura-2 measurement of cytosolic free Ca²⁺ in monolayers and suspensions of various types of animal cells. *J Cell Biol* **105**, 2145-2155 (1987).
158. L. D. Ly *et al.*, Oxidative stress and calcium dysregulation by palmitate in type 2 diabetes. *Exp Mol Med* **49**, e291 (2017).
159. S. Xu *et al.*, Palmitate induces ER calcium depletion and apoptosis in mouse podocytes subsequent to mitochondrial oxidative stress. *Cell Death Dis* **6**, e1976 (2015).
160. A. Akoumi, T. Haffar, M. Moustjerji, R. S. Kiss, N. Bousette, Palmitate mediated diacylglycerol accumulation causes endoplasmic reticulum stress, Plin2 degradation, and cell death in H9C2 cardiomyoblasts. *Exp Cell Res* **354**, 85-94 (2017).
161. B. N. Colvin, M. S. Longtine, B. Chen, M. L. Costa, D. M. Nelson, Oleate attenuates palmitate-induced endoplasmic reticulum stress and apoptosis in placental trophoblasts. *Reproduction* **153**, 369-380 (2017).
162. J. Kuzmicic *et al.*, Trimetazidine prevents palmitate-induced mitochondrial fission and dysfunction in cultured cardiomyocytes. *Biochem Pharmacol* **91**, 323-336 (2014).

163. W. Chang, L. Chen, G. M. Hatch, Berberine treatment attenuates the palmitate-mediated inhibition of glucose uptake and consumption through increased 1,2,3-triacyl-sn-glycerol synthesis and accumulation in H9c2 cardiomyocytes. *Biochim Biophys Acta* **1861**, 352-362 (2016).
164. Y. Ying, H. Zhu, Z. Liang, X. Ma, S. Li, GLP1 protects cardiomyocytes from palmitate-induced apoptosis via Akt/GSK3b/b-catenin pathway. *J Mol Endocrinol* **55**, 245-262 (2015).
165. T. Haffar, A. Akoumi, N. Bousette, Lipotoxic Palmitate Impairs the Rate of β -Oxidation and Citric Acid Cycle Flux in Rat Neonatal Cardiomyocytes. *Cell Physiol Biochem* **40**, 969-981 (2016).
166. X. Zhou, B. Chang, Y. Gu, MicroRNA-21 abrogates palmitate-induced cardiomyocyte apoptosis through caspase-3/NF- κ B signal pathways. *Anatol J Cardiol* **20**, 336-346 (2018).
167. J. Fauconnier *et al.*, Effects of palmitate on Ca(2+) handling in adult control and ob/ob cardiomyocytes: impact of mitochondrial reactive oxygen species. *Diabetes* **56**, 1136-1142 (2007).
168. J. Li, Y. Zhou, W. Zhang, C. Bao, Z. Xie, Relief of oxidative stress and cardiomyocyte apoptosis by using curcumin nanoparticles. *Colloids Surf B Biointerfaces* **153**, 174-182 (2017).
169. A. P. Landstrom *et al.*, Mutations in JPH2-encoded junctophilin-2 associated with hypertrophic cardiomyopathy in humans. *J Mol Cell Cardiol* **42**, 1026-1035 (2007).
170. Y. Matsushita *et al.*, Mutation of junctophilin type 2 associated with hypertrophic cardiomyopathy. *J Hum Genet* **52**, 543-548 (2007).
171. S. Minamisawa *et al.*, Junctophilin type 2 is associated with caveolin-3 and is down-regulated in the hypertrophic and dilated cardiomyopathies. *Biochem Biophys Res Commun* **325**, 852-856 (2004).
172. A. Guo *et al.*, Molecular Determinants of Calpain-dependent Cleavage of Junctophilin-2 Protein in Cardiomyocytes. *J Biol Chem* **290**, 17946-17955 (2015).
173. J. Hu *et al.*, RBFox2-miR-34a-Jph2 axis contributes to cardiac decompensation during heart failure. *Proc Natl Acad Sci U S A* **116**, 6172-6180 (2019).
174. J. Han, H. Wu, Q. Wang, S. Wang, Morphogenesis of T-tubules in heart cells: the role of junctophilin-2. *Sci China Life Sci* **56**, 647-652 (2013).
175. E. Kania, B. Pająk, A. Orzechowski, Calcium homeostasis and ER stress in control of autophagy in cancer cells. *Biomed Res Int* **2015**, 352794 (2015).
176. B. A. Ersoy, K. M. Maner-Smith, Y. Li, I. Alpertunga, D. E. Cohen, Thioesterase-mediated control of cellular calcium homeostasis enables hepatic ER stress. *J Clin Invest* **128**, 141-156 (2018).
177. J. K. Jin *et al.*, ATF6 Decreases Myocardial Ischemia/Reperfusion Damage and Links ER Stress and Oxidative Stress Signaling Pathways in the Heart. *Circ Res* **120**, 862-875 (2017).
178. L. Gong *et al.*, RTN1-C mediates cerebral ischemia/reperfusion injury via ER stress and mitochondria-associated apoptosis pathways. *Cell Death Dis* **8**, e3080 (2017).

179. A. Dandekar, R. Mendez, K. Zhang, Cross talk between ER stress, oxidative stress, and inflammation in health and disease. *Methods Mol Biol* **1292**, 205-214 (2015).
180. J. O. Reynolds *et al.*, Junctophilin-2 gene therapy rescues heart failure by normalizing RyR2-mediated Ca. *Int J Cardiol* **225**, 371-380 (2016).
181. W. Wang *et al.*, Reduced junctional Na⁺/Ca²⁺-exchanger activity contributes to sarcoplasmic reticulum Ca²⁺ leak in junctophilin-2-deficient mice. *Am J Physiol Heart Circ Physiol* **307**, H1317-1326 (2014).
182. S. Y. Li *et al.*, Cardiac contractile dysfunction in Lep/Lep obesity is accompanied by NADPH oxidase activation, oxidative modification of sarco(endo)plasmic reticulum Ca²⁺-ATPase and myosin heavy chain isozyme switch. *Diabetologia* **49**, 1434-1446 (2006).
183. E. Tuncay, E. N. Okatan, G. Vassort, B. Turan, β -blocker timolol prevents arrhythmogenic Ca²⁺ release and normalizes Ca²⁺ and Zn²⁺ dyshomeostasis in hyperglycemic rat heart. *PLoS One* **8**, e71014 (2013).
184. Y. Hattori *et al.*, Diminished function and expression of the cardiac Na⁺-Ca²⁺ exchanger in diabetic rats: implication in Ca²⁺ overload. *J Physiol* **527 Pt 1**, 85-94 (2000).
185. A. Zarain-Herzberg, G. García-Rivas, R. Estrada-Avilés, Regulation of SERCA pumps expression in diabetes. *Cell Calcium* **56**, 302-310 (2014).

Curriculum Vitae

Name: Xiaoyun Ji

Post-secondary Education and Degrees:

Western University
London, Ontario, Canada
2018-2019 MSc.

Jiangsu University
Zhenjiang, Jiangsu, China
2014-2016 MSc.

Jiangsu University
Zhenjiang, Jiangsu, China
2009-2014 BSc.

Honours and Awards:

Western Graduate Research Scholarship
2018-2020 Western University

National Scholarship for Graduate Students
2014-2015 Jiangsu University

Jiangsu University First Grade Scholarship
2014-2016 Jiangsu University

Jiangsu University Excellent Graduate Student Leader
2014-2016 Jiangsu University

National Encouragement Scholarship for Undergraduate Students
2009-2013 Jiangsu University

Jiangsu University First Grade Scholarship
2009-2013 Jiangsu University

Jiangsu University Excellent Student Leader
2011-2012 Jiangsu University

Top Ten Singers of Jiangsu University
2014 Jiangsu University

Related Work Experience Intern
The Affiliated People's Hospital of Jiangsu University
2013-2014

Publications:

Pathology and Laboratory Medicine Research Day, London, Ontario

Abstract accepted "Junctophilin-2 Protects Cardiomyocytes against Palmitate-induced Injury"

Poster presenting on January 8, 2019